Anonymous Referee #2

Received and published: 16 December 2011

This paper presents an extensive amount of data at three different sites, over a long time period, for Hg(0), RGM and Hg(P). This is an extraordinary and unique data set, and as such eventually warrants publication. The authors have done a considerable amount of work in analysing this data with respect to meteorological and atmospheric physical parameters. This work is reflected in the draft, and the quality of this work is high.

Despite this rich data set, however, the scientific conclusions and insights drawn from the paper are weak at best. This to some extent reflects the state of the field – we don't understand the variation of mercury species with meteorology – and this extensive data set and analytical work proves the point. At best, the authors nibble around the edges of this question, listing tentative associations.

I struggled even as an expert reader to glean scientific insights that might be broadly relevant from this paper, which raises the question of whether there is enough content here to be of broader interest to the ACP reader. In a revision, I would like to see the authors be a bit more ambitious in identifying the key take-home messages from this rich data set. Perhaps given the uncertainty these can be presented as hypotheses to be tested. But as is, the interpretation of the associations presented is almost totally missing. To this end, the authors also need to dramatically improve the presentation and writing of the paper (and limit the number of figures to n«17).

Per reviewers' suggestions, we have made extensive revisions to the content, structure and writing of the manuscript. We added Section 4, with a summary of key results in Table 5, to emphasize the idiosyncrasies in the relationships mercury species possibly had with physical parameters in three different geographic environments, to discuss unique points from this study in comparison to previous work, and to hypothesize on possible mechanisms controlling those relationships. Please see the revised manuscript.

Specific comments follow:

general: Would it help to look at multivariate correlations (ie temp and precip together) using more advanced statistical methods?

We set out with similar ideas in mind. However, after a careful examination of the relationships between speciated mercury and individual climate variables, we decided not to pursue it because what we found was tendencies, not one-to-one data point corresponding relationships between two variables, and it would take a more focused and in-depth study to uncover better-defined relationships in sub-datasets which can simplify atmospheric conditions by the predominant

effects of one variable at the time. With this study being as exhaustive as is in its present form, we will have to pursue that in the future.

p 28402 line 15: This sort of structure – where a tentative insight is presented, then methods for follow up, then another insight – contributes to confusion in reading this paper. I would suggest that data analysis methods would be appropriately placed in methods, results in results, and discussion in discussion.

Per reviewers' suggestions, we have made extensive revisions to the content, structure and writing of the manuscript. Now we added Section 4, with a summary of key results in Table 5, to emphasize the idiosyncrasies in the relationships mercury species possibly had with physical parameters in three different geographic environments, to discuss unique points from this study in comparison to previous work, and to hypothesize on possible mechanisms controlling those relationships. Please see the revised manuscript.

p 28403 line 15-20: is there any way to go beyond this speculation and quantitatively assess these differing conditions? Filtering the data? etc.

This paragraph has been revised with more analysis added. Please see Lines 229 - 244 in the revised manuscript. It is also included as follows:

"At TF (coastal) 50% of the total data were collected under wind speed <1 m s^{-1}, which nearly all occurred at night (00:00 – 11:00 UTC) and before noon local time (12:00-17:00 UTC), and over this range of wind speed, the median and 75th percentile values were lowest. The largest 75th percentile value (0.6 ppqv) was associated with wind speed 2 – 3 m s^{-1}. Overall, under conditions of wind speed > 2 m s^{-1}, nearly 90% of the data points were collected during the day (12:00 – 23:00 UTC) and before midnight local time (00:00 – 05:00 UTC), and over half of the data points were sampled in the afternoon local time (18:00 – 23:00 UTC). The implications of these features are twofold. First, higher RGM levels were possibly a result of local production and transport. Second, there are opposing effects of windier conditions on the ambient level of RGM at TF (coastal), increased dry depositional loss and enhanced transport of RGM. In addition, stronger winds are often associated with precipitation resulting in scavenging via wet deposition. The wind rose of RGM (Figure 4b) showed that mixing ratios over 0.6 – 3 ppqv occurred in all wind directions except over the ranges of 330° – 360° and 0° – 45°. RGM >3 ppqv occurred in two ranges: southeasterly (~135°) and southerly to northwesterly (180°-315°), which have been proved in our previous studies to be the flow regimes that facilitated pollutant transport from sources in the Northeast (Mao and Talbot, 2004b)."

p 28404 line 14: Another possibility is that deposition via sea salt aerosols is a) reversible or b) slow.

This point and relevant reference are added into text now as follows:

"Further, it could also result from release of RGM in the form of $HgCl_2$ from the surface of sea salt aerosols as suggested by Pirrone et al. (2000) and the several days lifetime of sea salt aerosols."

See Lines 567 - 569 in the revised manuscript.

p 29404 line 24: Is there any quantitative basis (back-trajectory modeling, for example) that could back this up? As is, it reads as if the authors are just guessing. It would be easy to check, for example, for the days in question using HYSPLIT.
Section 3.2 solar radiation: what impact does potential emission from the surface (either land or sea) have?

We ran three-day backward trajectories at the 500 m, 1000 m, and 2000 m altitude for air masses with high Hg^P levels during the time period, i.e. 4 February – 15 March 2009, and found that those air masses originated from southern Canada or eastern to southern U.S. states via sweeping southerly to northwesterly flows at the three altitudes. The same back trajectories run for air masses with low Hg^P levels during the same time period did not appear to be vastly different. We added this piece of information in the text as follows:

"The relationship between Hg^P and wind speed at TF (coastal) suggested no dependence of all metrics of Hg^P, including 25^{th} percentile, median, or 75^{th} percentile values, on wind direction over all ranges of wind speed (Figures 5a,b). A handful of data greater than 1 ppqv turned out to be collected exclusively on several days over 4 February – 15 March 2009 coming from southeast to northwest. Such levels of Hg^P were hardly observed beyond that season. Three-day backward trajectories suggested that air masses with higher Hg^P levels originated from southern Canada or eastern to southern U.S. via sweeping southerly to northwesterly flows from the 500 m to 2000 m altitude. The same back trajectories run for air masses with low Hg^P levels during the same time period did not appear to be vastly different. It is unclear why the highest Hg^P mixing ratios were measured during winter 2009."

Please see Lines 263 – 272 in the revised manuscript.

p 28406 line 23-25: these are very low r2 values. Is this significant?

The lines represent the 95% confidence interval.

These correlations are the best defined from all the correlations between speciated mercury and climate variables, especially in the case of one-to-one corresponding plots.

p 28408, line 8-10: doesn't the fact that it ranks 104/116 mean that it was an exceptionally cold, dry February? I'm not exactly sure what point is being made here.

The ranking is in an ascending order regarding temperature and precipitation amount. The text is revised as follows:

"February 2010, which was ranked as the 104th February from 1st being the coldest to 116th warmest and 104th from 1st driest to 116th wettest in New Hampshire based on the 116 years of record running from 1895 to 2010 (http://www.nrcc.cornell.edu/page_summaries.html)."

See Lines 332 – 336.

We tried to make a point that more RGM was possibly washed out by more rain water (as opposed to snow) in a warm winter such as winter 2010, and therefore we saw RGM levels hovering around the LOD during that winter.

Speciated Mercury at Marine, Coastal, and Inland Sites in New England: Part II. Relationships with Atmospheric Physical Parameters

Huiting Mao[1], Robert Talbot[2], Jennifer Hegarty[3], and James Koermer[4]

[1]Department of Chemistry, State University of New York, College of Environmental Science and Technology, Syracuse, NY 13219, USA
[2]Department of Earth and Atmospheric Sciences, University of Houston, Houston, TX 77204, USA
[3]AER, Inc., 131 Hartwell Avenue, Lexington, MA, 02421, USA
[4] Department of Atmospheric Science & Chemistry, Plymouth State University, Plymouth, New Hampshire 03264

Contact Info:

hmao@esf.edu
315-470-6823

Submitted to:
Atmospheric Chemistry and Physics
for Special Issue titled "Atmospheric Mercury Processes: Papers from the 10th ICMGP"

Revised and submitted on January 3, 2012

Abstract

Long-term continuous measurements of gaseous elemental mercury (Hg°), reactive gaseous mercury (RGM), and particulate phase mercury (Hg^P) were conducted at coastal (Thompson Farm, denoted as TF), marine (Appledore Island, denoted as AI), and elevated inland (Pac Monadnock, denoted as PM) monitoring sites of the AIRMAP Observing Network. Diurnal, seasonal, annual, and interannual variability in Hg°, RGM, and Hg^P from the three distinctly different environments were characterized and compared in Part I. Here in Part II relationships between speciated mercury (i.e., Hg^o, RGM, and Hg^P) and climate variables (e.g., temperature, wind speed, humidity, solar radiation, and precipitation) were examined. The best point-to-point correlations were found between Hg^o and temperature in summer at TF and spring at PM, but there was no similar correlation at AI. Subsets of data demonstrated regional impacts of episodic dynamic processes such as strong cyclonic systems on ambient levels of Hg^o at all three sites, possibly through enhanced oceanic evasion of Hg°. A tendency of higher levels of RGM and Hg^P was identified in spring and summer under sunny conditions in all environments. Specifically, the 10^{th}, 25^{th}, median, 75^{th}, and 90^{th} percentile mixing ratios of RGM and Hg^P increased with stronger solar radiation at both the coastal and marine sites. These metrics decreased with increasing wind speed at AI indicating enhanced loss of RGM and Hg^P through deposition. RGM and Hg^P levels correlated with temperature positively in spring, summer and fall at the coastal and marine locations. In the coastal region relationships between RGM and relative humidity suggested a clear decreasing tendency in all metrics from <40% to 100% relative humidity in all seasons especially in spring, compared to less variability in the marine environment. The effect of precipitation on RGM at coastal and marine locations was similar. At the coastal site, RGM levels were a factor of 3-4 to two orders of magnitude higher under dry

57 conditions than rainy conditions in all seasons. In winter RGM mixing ratios appeared to be
58 mostly above the limit of detection (LOD) during snowfalls suggesting less scavenging
59 efficiency of snow. Mixing ratios of Hg^P at the coastal and marine sites remained above the
60 LOD under rainy conditions. Precipitation had negligible impact on the magnitude and pattern of
61 diurnal variation of Hg^P in all seasons in the marine environment.
62

1. Introduction

Mercury is a dangerous toxin detrimental to human health and thus it is of paramount importance to understand the processes that control the ambient levels of atmospheric mercury. Mercury exists in three forms, gaseous elemental mercury (Hg^o), reactive gaseous mercury (RGM = $HgCl_2$ + $HgBr_2$+ HgOBr + …), and particulate phase mercury (Hg^p). Mercury cycling, i.e., transformation between the three forms, is intricately linked to dynamical, physical and chemical processes in the atmosphere. Moreover, source and sink strengths of Hg° are dependent on physical parameters such as temperature and wind. However, Jacob and Winner (2008) pointed out that the effect of long-term changing physical parameters (i.e., climate changes) on mercury cycling has received no attention to date.

Previous research has been conducted to examine the relationships between mercury and physical variables over a limited time period ranging from days to one or two years, which appeared to vary greatly at various geographic locations. For example, Gårdfeldt et al. (2003) found from their one month campaign over the Atlantic and two month measurements over the Mediterranean Sea that mercury evasion from sea water depended on temperature, wind, and salinity. Han et al. (2004) attributed a negative correlation between total gaseous mercury (TGM) and temperature to seasonal difference in emission rates of coal-fired power plants (winter maximum) in the northern hemisphere based on two summers of measurement data. A negative correlation between temperature and TGM was shown by measurements during a winter month at a rural site in the central Pearl River Delta region (Li et al., 2011). A ten month data set at Elora, Ontario, Canada suggested highest Hg^o concentrations in late spring and fall possibly due to increases in air temperature among other factors in spring and lower atmospheric mixing height in fall (Baya and Van Heyst, 2010). This relationship was supported by our study (Sigler

et al., 2009a) with significant positive correlation between seasonally averaged Hg^o and temperature in spring and fall 2007 at a coastal and marine site from southern New Hampshire. Ambient levels of Hg^o and TGM were also found to be correlated with solar radiation, relative humidity, and planetary boundary layer height (Cobbetta et al., 2007; Stamenkovic et al., 2007).

Reactive mercury was reportedly linked to temperature, radiation, humidity and precipitation. Sigler et al. (2009a) presented a positive relationship between seasonal averaged RGM and temperature at a coastal site whereas none from the marine site. Transformation from Hg^o to RGM by oxidation involves photochemistry (Lin et al., 1999), which indicates a link between RGM concentrations and solar radiation. Indeed, studies have shown the diurnal patterns of RGM and radiation flux were close in phase (Mason and Sheu, 2002; Spovieri et al., 2003; Sigler et al., 2009a). Laurier et al. (2003) observed the concurrence of highest RGM and maximum UV radiation flux in the marine boundary layer over the North Pacific Ocean. Highest RGM levels were observed around midday after nights of high relative humidity, while lowest concentrations were found during high relative humidity and rainfall (Mason and Sheu, 2002; Laurier et al. 2003; Poissant et al., 2004; Poissant et al., 2005; Laurier et al., 2007).

There are limited long-term data sets of Hg^P, and their relationships with physical variables suggested that high levels were mostly associated with wind driven transport, chemical and physical transformation processes. For instance, the one-year Hg^p dataset from Poissant et al. (2005) exhibited higher levels of Hg^P associated with transport, RGM gas-particle partitioning, and Hg^o oxidation. Liu et al. (2007) suggested that the diurnal pattern of Hg^P (as well as that of Hg^o) was strongly influenced by boundary layer dynamics, temperature and humidity based on their one year measurements in Detroit, MI. Similarly, Brooks et al. (2010) found that during a summer campaign in Houston, TX, peaks of Hg^P (as well as Hg^o and RGM) showed distinct and

consistent relationships with the average planetary boundary layer dynamics, which were enhanced in a shallow nocturnal boundary layer.

Wind data have been used to trace back the origin of high mercury concentrations. Some studies often found association between high concentrations of mercury and wind direction which points to upwind source regions (e.g. Gabriel et al., 2005; Poissant et al., 2005; Aucott et al., 2009; Sigler et al., 2009a; Baya and van Heyst, 2010), while others detected no correlation (Castillo et al., 2011). In addition, our previous study found a relationship between wind speed and possible oceanic evasion (Sigler et al., 2009b). We hypothesized the impact of the April 2007 Nor'easter on ambient levels of Hg^o that were reflected in sudden enhancements of 52 ppqv and 26 ppqv over a span of 14 and 12 hours at a coastal and inland site, respectively.

While long-term studies of TGM have been conducted, few studies have been dedicated to the investigation of long-term relationships between speciated mercury and physical parameters. Six-year measurement datasets from Mace Head, Ireland and Zingst, Germany showed a strong positive correlation TGM bore with wind and dew point (Kock et al., 2005). Cole and Steffen (2010) found a positive correlation between Hg^o and air temperature from their 12 year (1995 – 2007) measurement data in Alert, Canada although it was not clear if temperature was the direct cause of the Hg^o variability. Multiple-year continuous measurements of Hg°, RGM, and Hg^P have been conducted at inland, coastal, and marine locations from the AIRMAP Observing Network. This study is Part II of a two paper series. Part I focuses on key characteristics of Hg°, RGM, and Hg° variations ranging from diurnal to interannual time scales and their differences between locations with distinct geographical characteristics (Mao and Talbot, 2011). In this study we investigated how the three forms of mercury are associated with atmospheric conditions via their relationships with climate variables in different environments.

2. Measurements and Approach

As stated in Mao and Talbot (2011), multiple-year measurements of Hg°, RGM, and Hg^P have been conducted at three AIRMAP (www.airmap.unh.edu) Observatory sites: Thompson Farm (43.11°N, 70.95°W, 24 m agl) (TF), Pac Monadnock (42.86°N, 71.88°W, 700 m agl) (PM), and Appledore Island (42.97°N, 70.62°W, 40 m agl) (AI). The PM and TF sites are 185 and 25 km, respectively, inland from the Atlantic Ocean, while AI is 10 km offshore in the Gulf of Maine. The locations of the three sites form a unique west-east oriented transect with site surroundings composed of heavily forested, coastal, and marine boundary layer environments. Moreover, due to the remote central location of PM in New England and its 700 m elevation (i.e., above the nocturnal inversion and in the middle of the daytime boundary layer), the site is ideally located to determine regional trends in trace gases, including mercury (Mao and Talbot, 2004; Mao et al., 2008).

Mercury instruments were operated in a manner identical at TF (coastal), PM (inland), and AI (marine) to ensure data consistency. Details of the instruments can be found in Mao et al. (2008), Sigler et al. (2009a), and Mao and Talbot (2011). Briefly, a Tekran 1130 denuder module operated in series with the 2537A provided continuous measurements of RGM and Hg° respectively. Ambient mixing ratios of Hg° were measured continuously using the 2537A cold vapor atomic fluorescence spectrometer with 5-minute time resolution and a limit of detection (LOD) of ~10 ppqv (1 ng m^{-3} = 112 ppqv). RGM is measured with a 90 minute sampling interval yielding a LOD of ~0.1 ppqv based on three times the standard deviation of the field blank values determined at TF (coastal) during 2007. The inlet of the Tekran 1135 for measuring Hg^P at AI (marine) was modified by replacing the elutriator with one that contained

154 no impaction plate to facilitate collection of coarse aerosols on the quartz frit in the Tekran 1135
155 (Talbot et al., 2011).

156 Continuous Hg° measurements with 5-minute resolution have been ongoing since
157 November 2003 at TF (coastal), December 2004 at PM (inland), and June 2007 at AI (marine).
158 Measurements of RGM with 2-hour resolution were added at TF (coastal) in November 2006,
159 December 2006 at PM (inland), and on AI (marine) in June 2007. Measurements of Hg^P started
160 at TF (coastal) in February 2009 and on AI (marine) in April 2009.

161 Data of temperature, wind, relative humidity, solar radiation (in the form of JNO_2 at AI
162 (marine)) were obtained from the long term meteorological measurements by AIRMAP at TF
163 (coastal), PM (inland), and AI (marine). This is complemented by hourly precipitation and
164 radiation flux data from the NOAA's US Climate Reference Network site co-located at TF
165 (coastal) (publicly available at http://www.ncdc.noaa.gov/crn/products.html), as well as 6-hourly
166 precipitation data from NOAA's National Weather Service site at Pease, NH which is the closest
167 approximation for data on AI (marine). Where there were a significant fraction of wind and
168 temperature data missing on AI (marine) due to power shortage under extreme weather
169 conditions, GoMOOS meteorological data from the site on Star Island was used as substitute.
170 The two islands were merely a few tens meters apart and their overlapping data of temperature
171 and wind were verified to be correlated at $r^2>0.9$. GoMOOS data are publicly available
172 (http://www.gomoos.org/data/recent.html).

173 Measurement data of carbon monoxide (CO) were used in this study in determining
174 anthropogenic influence. A detailed study of relationships between Hg^o/RGM/Hg^P and other
175 chemical compounds will be presented in Part III (Mao et al., 2012). A description of CO
176 measurement can be found in Mao and Talbot (2004a).

3. Relationships between Hg°/RGM/Hg^P and meteorological parameters

3.1 Wind

One of the most significant sources of mercury is anthropogenic emissions, and the AIRMAP Observing Network is located downwind of major industrial sources and metropolitan areas. Moreover, Sigler et al. (2009b) reported enhancements of 30-50 ppqv in Hg° mixing ratios at TF a coastal and at PM (inland) an elevated inland site in southern NH during the most intense period of the April 2007 Nor'easter and hypothesized that it was due to strong wind induced oceanic emissions. Therefore, it is logical to speculate on an association between Hg° levels and wind speed and direction. Yet, seasonal scatter plots of Hg° mixing ratios versus wind speed and directions at TF (coastal), AI (marine), and PM (inland) did not reveal distinct relationships.

However, a close examination of a subset of data revealed association between Hg° mixing ratios and wind speed at AI (marine), as suggested in Figure 1a, where the majority of the measurements were taken during the time periods of 22 – 29 October and the month of November 2008. Interestingly there appeared to be a 3-4 day periodicity in Hg° mixing ratios during the time period of 22 October – 30 November 2008 (Figure 1a). Some periods of higher Hg° levels coincided with higher CO levels and others showed Hg° and CO in opposite phases. A particular interesting case is the one over 14-16 November 2008, when Hg^o and wind speed was correlated at r^2=0.18 and slope = 3.7 ppqv per m s^{-1} (Figures 1b,c). The Hg° mixing ratio started increasing in the early morning and was enhanced by ~70 ppqv reaching 205 ppqv in 24 hours, and this increase, somewhat dampened later on, lasted through midday 16 November. During the hours of the first Hg° peak on 15 November CO measurements were not available; during the hours of the second Hg° peak on 16 November, CO mixing ratios were decreased by

200 ~40 ppbv to as low as ~90 ppbv at 00:00. The wind direction appeared to be varying in the two
201 easterly quadrants and was mostly southerly and southeasterly at the times of the CO minimum
202 and Hg° maximum. This indicates that the increase of Hg° on 16 November was likely
203 influenced by an influx of air from the relatively clean oceanic region.

204 To support our speculation, we examined the dynamic patterns during 14-16 November
205 2008. During this time period New England was impacted by a strong cyclone with sustained
206 coastal surface winds exceeding 15 m s^{-1} and periods of widespread heavy rainfall. At 00:00
207 UTC on 16 November the cyclone was located in upstate New York near the Canadian border
208 with a central sea level pressure of 990 hPa (Figure 2) and produced strengthening southerly and
209 southeasterly surface winds at AI (marine) and surrounding coastal and marine locations during
210 the afternoon of 15 November and into the morning of 16 November. The wind speed measured
211 at AI (marine) increased from ~3 m s^{-1} at 00:00 UTC on 15 November to ~8 m s^{-1} in 12 hours,
212 then after a slight slowing during that afternoon increased steadily to a peak value greater than 16
213 m s^{-1} by 00:00 UTC on 16 November. The winds at AI (marine) shifted into the southwesterly
214 and then northwesterly direction during the day on 16 November before gradually slowing
215 during the next day as the cyclone center moved northeastward into eastern Canada. The
216 evolution of dynamic processes during 14 – 16 November suggested unusually strong winds
217 from a maritime direction that coincided in time with the onset of the sudden increase in Hg°.

218 We also examined Hg° mixing ratios during the same time period for TF (coastal) and
219 PM (inland) (Figure 3). Prior to the storm there were distinct diurnal cycles at TF (coastal) with
220 the daily maximum in the late afternoon followed by a steady decrease to the daily minimum
221 before sunrise. On 13 November the Hg° mixing ratio kept rising after reaching the daily
222 maximum and the increasing trend continued through 14 November leveling off at 173 ppqv on

15 November and then hovered around that level until 12:00 UTC of 16 November (Figure 3a). PM (inland) experienced an increase during 14 – 15 November that was similar to the one at TF (coastal) followed by a slowed decrease on 15 November (Figure 3b). These somewhat synchronized changes in Hg° mixing ratios at the three sites during the storm supported our hypothesis in Sigler et al. (2009b) that strong wind induced enhancement in oceanic emissions of Hg° can have a regional influence on ambient levels of Hg° that can reach far inland.

At TF (coastal) 50% of the total data were collected under wind speed <1 m s^{-1}, which nearly all occurred at night (00:00 – 11:00 UTC) and before noon local time (12:00-17:00 UTC), and over this range of wind speed, the median and 75th percentile values were lowest. The largest 75th percentile value (0.6 ppqv) was associated with wind speed 2 – 3 m s^{-1}. Overall, under conditions of wind speed > 2 m s^{-1}, nearly 90% of the data points were collected during the day (12:00 – 23:00 UTC) and before midnight local time (00:00 – 05:00 UTC), and over half of the data points were sampled in the afternoon local time (18:00 – 23:00 UTC). The implications of these features are twofold. First, higher RGM levels were possibly a result of local production and transport. Second, there are opposing effects of windier conditions on the ambient level of RGM at TF (coastal), increased dry depositional loss and enhanced transport of RGM. In addition, stronger winds are often associated with precipitation resulting in scavenging via wet deposition. The wind rose of RGM (Figure 4b) showed that mixing ratios over 0.6 – 3 ppqv occurred in all wind directions except over the ranges of 330° – 360° and 0° – 45°. RGM >3 ppqv occurred in two ranges: southeasterly (~135°) and southerly to northwesterly (180°-315°), which have been proved in our previous studies to be the flow regimes that facilitated pollutant transport from sources in the Northeast (Mao and Talbot, 2004b).

Compared to TF (coastal), winds were stronger at AI (marine), and RGM mixing ratios

246 appeared to be less dependent on wind speed, which is evidenced in median values of 0.2 ppqv
247 in all wind speed ranges except the median value below the LOD for wind speed greater than 10
248 m s^{-1} (Figure 4c). The 75th percentile value varied from 0.3 ppqv at winds exceeding 10 m s^{-1} to
249 0.6 ppqv at winds <6 m s^{-1}. RGM at AI is a result of Hg° oxidation, transport, and deposition, of
250 which the net effect seemed to be most positive to the ambient level over the <6 m s^{-1} wind speed
251 range. The wind rose (Figure 4d) suggested that the majority of RGM mixing ratios >1 ppqv
252 were observed in all directions, but the few ones >4 ppqv, which occurred in spring, were mostly
253 from the south and the west, whose upwind source regions are the greater Boston area and
254 southern NH.

255 At PM (inland) median values of RGM mixing ratios in all wind ranges remained
256 consistently below the LOD; the 75th percentile values barely reach the LOD (Figure 4e). The
257 majority of RGM mixing ratios >0.2 ppqv were observed in two primary wind direction ranges,
258 east and southwest (Figure 4f) in the four seasons of 2007, with a few samples from the southeast.
259 There are two coal-fired power plants southwest of PM (inland) near Springfield, MA (Solution,
260 Inc and Northeastern Utilities), one southeast of PM (inland) in Salem, MA (Dominion Salem
261 Harbor), and two east of PM (inland) in NH. Possibly on days with favorable wind conditions
262 influence of these power plant emissions could reach PM (inland).

263 The relationship between Hg^P and wind speed at TF (coastal) suggested no dependence of
264 all metrics of Hg^P, including 25th percentile, median, or 75th percentile values, on wind direction
265 over all ranges of wind speed (Figures 5a,b). A handful of data greater than 1 ppqv turned out
266 to be collected exclusively on several days over 4 February – 15 March 2009 coming from
267 southeast to northwest. Such levels of Hg^P were hardly observed beyond that season. Three-day
268 backward trajectories suggested that air masses with higher Hg^P levels originated from southern

Canada or eastern to southern U.S. via sweeping southerly to northwesterly flows from the 500 m to 2000 m altitude. The same back trajectories run for air masses with low Hg^P levels during the same time period did not appear to be vastly different. It is unclear why the highest Hg^P mixing ratios were measured during winter 2009.

Unlike the TF (coastal) location, at AI (marine) there appeared to be a decreasing tendency in Hg^P mixing ratios with increasing wind speed (Figure 5c). In particular, the 75th percentile value decreased from 0.6 ppqv at wind speed <6 m s^{-1} to 0.2 ppqv at wind speed >10 m s^{-1}, and the trend in median values for all wind speed ranges was similar but the decrease rate was slowed by one-half. This suggests a strong impact of dry depositional loss of aerosols on ambient mixing ratios. For samples with Hg^P >1.5 ppqv, air masses seemed to come from all directions, whereas air with Hg^p over the range of 0.5 – 1.5 ppqv was more prevalent in the westerly flow indicating a land influence (Figure 5d).

3.2 Solar radiation

The relationship of Hg°, RGM, or Hg^P with solar radiation was examined using Hg°, RGM, or Hg^P versus surface solar radiation flux at TF (coastal) while versus jNO_2 at AI (marine) for daytime: 12:00 – 18:00 UTC and 18:00 – 00:00 UTC. No measurements of solar radiation were available at PM (inland). No relationship between Hg° and solar radiation was observed at TF (coastal) and AI (marine) for the two daytime quadrants in all seasons, and thus we focus on RGM and Hg^P.

For RGM at TF (coastal), a positive relationship with solar radiation in spring was observed in the 25th, median, and 75th percentile values, while at AI (marine) a positive relationship was found in both spring and summer (Figures 6a,b). The increase with radiation flux was more significant at TF (coastal) with the median value rising from 0.4 to 1.4 ppqv

compared to a lesser increase from 0.1 to 0.4 ppqv at AI (marine). For Hg^P, its positive relationship with solar radiation was observed in summer at both TF (coastal) and AI (marine) (Figures 6c,d). One exception is that at AI (marine), the increasing trends in the 25th, median, and 75th percentile values of Hg^P turned downward at jNO_2 >0.008 s^{-1}. These results indicate that production processes of RGM and Hg^P are closely linked to solar radiation in the coastal and marine environments in spring and/or summer.

3.3 Temperature

Examination of seasonal data of Hg^o versus temperature at TF (coastal) indicated a scattered, correlative relationship between Hg^o and temperature in all summers during the time period of 2004 – 2010 (Figure 7) whereas no correlation appeared to exist in other seasons. The r^2 value varied over the range of 0.12 – 0.20 with slope values over 0.7 – 2.0 ppqv/ºC at the 95% confidence interval. At PM (inland) the Hg^o versus temperature at PM (inland) exhibited a somewhat positive correlation in springs 2007 – 2010 (Figure 8). At AI (marine), no correlation between Hg^o and temperature was found for all seasons during 2007 – 2010. One curious exception is winter 2009 where we found a correlation of r^2=0.2 and a 1.2 ppqv/ ºC slope value at the 95% confidence interval, and this correlation was not reproduced in the following winter.

In summary these relationships suggested a somewhat positive correlation between Hg^o and temperature in spring at a remote rural location situated above the boundary layer half of the time and in summer at a sea level coastal site, whereas no such correlation was found at a site in the marine boundary layer. The positive correlation at the former two sites was reproducible during the study period of 4 – 7 years with slightly varying correlation coefficients and slope values, which indicates the consistency of the relationship.

The box plot of RGM versus temperature at TF (coastal), PM (inland), and AI (marine)

315 suggested higher levels of RGM, be it the 25th percentile, median, or 75th percentile value, at
316 warmer temperatures during the warm season (i.e., spring and summer) and this tendency was
317 enhanced for daytime data (Figures 9, PM not shown). At TF (coastal), in spring the majority of
318 RGM mixing ratios >2 ppqv occurred at temperature >9^{o}C, and 10% of the daytime data in the
319 highest temperature bin (>18^{o}C) had mixing ratios >5 ppqv (Figure 9a). In summer, daytime
320 data for temperatures <21^{o}C had median levels below the LOD, and the median showed a
321 distinct increase from around the LOD over the temperature bin 21-24^{o}C to 0.3 ppqv for
322 temperatures >27^{o}C (Figure 9b). Wintertime data showed no discernible pattern; in the fall,
323 median values were below the LOD in all temperature bins except the highest one (>18^{o}C)
324 where it barely reached the LOD.
325 Similar to TF (coastal), larger RGM levels corresponded to higher temperatures in the
326 marine boundary layer based on measurements at AI (marine), and this relationship was
327 enhanced in daytime data (Figures 9c,d). In fall, only in the highest temperature bin (>16°C) did
328 the median level of ~ 0.3 ppqv exceed the LOD, and there was no systematic pattern in the 75th
329 percentile value. One unique feature at AI (marine) was that in winter higher median values (0.2
330 – 0.3 ppqv) were found in the temperature bins -6 – 0^{o}C while hovering around the LOD in
331 temperature bins below -6^{o}C or above 0^{o}C (Figure 9e). This pattern was slightly enhanced in
332 the daytime and lessened at night. Close examination revealed that 68% of the wintertime RGM
333 samples below the LOD were collected in February 2010, which was ranked as the 104th
334 February from 1st being the coldest to 116th warmest and 104th from 1st driest to 116th wettest in
335 New Hampshire based on the 116 years of record running from 1895 to 2010
336 (http://www.nrcc.cornell.edu/page_summaries.html). This implies that more RGM was possibly

337 washed out by rain water, as opposed to snow, in a warm winter season such as 2010. More
338 wintertime data in the future is needed to verify this hypothesis.

339 At PM (inland) the median and even the 75th percentile values rarely exceeded the LOD
340 and thus the box plot of RGM vs. temperature at PM is not shown. However, there were two
341 exceptions: 1.) in spring the median barely reached the LOD and the 75th percentile values rose
342 to 0.3 – 0.4 ppqv as temperature went beyond 8^{o}C, and 2.) in winter the 75th percentile value
343 varied over 0.1 – 0.2 ppqv in all temperature bins with an increasing tendency at warmer
344 temperatures.

345 Relationships between Hg^P and temperature were examined for TF (coastal) and AI
346 (marine) where measurements were available. At TF (coastal) total measurement data showed
347 two opposite regimes in the Hg^P-temperature relationship: negative and positive correlation at
348 temperatures below and above 8^{o}C, respectively (Figure 10a). Similar to RGM, Hg^P exhibited
349 an increasing tendency with warming temperatures in spring and summer, especially during
350 daytime at TF (coastal) (Figures 10b,c), which was consistently evidenced in the tendency of
351 nearly all of the median, 75th, and 90th percentile values. The magnitude of such tendency was
352 an increase of ~0.3 ppqv from the lower to upper end of temperature range (about 15°C
353 difference). In winter the tendency was reversed with the highest median and 75th values
354 corresponding to the lower temperatures (<-6°C) (Figure 10d), and this tendency was enhanced
355 in the nighttime data. The decrease in median and 75th percentile values was around 0.7 ppqv
356 from <-8°C to >2°C of temperature. In the fall, the median and 75th percentile values over all
357 temperature bins hovered around the LOD except at the upper end of the temperature range
358 (>17°C) with Hg^P reaching 0.3 – 0.4 ppqv which occurred mostly close in time to the warm
359 season.

At AI (marine) there was only one month of data for the winter season during the study period, and thus the Hg^P versus temperature relationship for all data largely represents the relationship in spring, summer and fall. Temperature ranged from <6°C to >21°C, much narrower than at TF (coastal), due in part to the marine climate. Perhaps because of the missing wintertime data, there is only one pattern showing in all metrics, which is that the 10^{th}, 25^{th}, median, 75^{th}, and 90^{th} percentile values increased with warming temperature (Figure 11a). This tendency was enhanced in spring and summer (Figures 11b,c). In the fall, the median values exceeded the LOD at temperatures <10°C and temperatures >16°C; the latter was primarily close in time to the warm season (Figure 11d).

3.4 Relative Humidity

No overall well-defined relationships were observed between Hg^o and relative humidity at TF (coastal), PM (inland), and AI (marine) for all seasons. Two points are noted. First, at TF (coastal), in summer and fall there were very low levels of Hg^o, reaching as low as 40 – 50 ppqv corresponding to 95-100% relative humidity, which occurred on nights with nocturnal inversions. Second, in summer at AI (marine) there appeared to a linear upper boundary enveloping the data, which was reproduced in the three summers (2007, 2008, and 2010) with available relative humidity data (Figures 12a,b,c).

A close examination of the upper boundary in the summertime data at AI (marine) revealed that nearly all samples were collected in the month of August during those three summers. Specifically, August data comprised 93% of the data forming the upper boundary, and these data points did not suggest preferential time quadrants of the day. Corresponding to these data points, there was a vague anti-correlation between Hg^o and temperature as well as between temperature and relative humidity (Figures 12d,e,f,g). In the meantime no systematic patterns

383 were observed between Hg^o and JNO_2, as well as between JNO_2 and temperature. It indicates
384 that solar radiation may not be the dominant driving force for the linear relationship between Hg^o
385 and relative humidity in August; it may result from the dominance of thermal processes in the
386 marine boundary layer during that time of a year. Future research is warranted to understand the
387 driving mechanism for this curious linearity in August.

388 Relationships between RGM and relative humidity at TF (coastal) suggested a clear
389 decreasing tendency in all metrics, including 10^{th}, 25^{th}, median, 75^{th}, and 90^{th} percentile values,
390 from less than 40% to 100% relative humidity levels in all seasons (Figures 13a-e). Particularly
391 in spring, the median level of RGM was 1 ppqv, 75^{th} and 90^{th} percentile values were nearly 2 and
392 4 ppqv respectively for relative humidity <40%, followed by a steep decrease over the 50-60%
393 range and a continuous decrease to a median level below the LOD over the 90-100% range.
394 Similar patterns were found in all other seasons. At PM (inland), only in spring and winter for
395 relative humidity below 60% the median level of RGM exceeded the LOD.

396 The largest difference in RGM versus relative humidity at AI (marine) (Figures 13f-j)
397 compared to TF (coastal) and PM (inland) was less variability of the metrics, except the 90^{th}
398 percentile value, over all bins of relative humidity. Specifically, in the overall relationship
399 (Figure 13f) the 25^{th}, median, and 75^{th} percentile values varied over a narrow range of 0.17 –
400 0.36 ppqv except the 90-100% bin where the median was below the LOD. Another difference
401 was the highest levels of RGM, represented in metrics, were observed in summer for relative
402 humidity <50% compared to the highest levels of RGM occurring in spring at TF (coastal).

403 The plots of RGM versus relative humidity for TF (coastal) suggested a better defined
404 negative correlation in spring and summer (r^2=0.25 and 0.30 respectively) than in fall and winter
405 (Figure 14). Since at night humidity reaches >90% most of the time and removal of RGM and

406 Hg^P is rapid, we will consider the relationship for daytime only (i.e., 12:00 – 23:59 UTC) and no
407 precipitation. Fifteen percent of the total 1336 samples during the four springs exceeded 2 ppqv
408 which corresponded to relative humidity <60%. In the four summers, 20% the total 1395
409 samples exceeded 0.5 ppqv corresponding to relative humidity varying over 40%-100% with the
410 largest under drier conditions gradually decreasing to wetter conditions. Faïn et al. (2009)
411 showed that high RGM levels were always observed with relative humidity below 40 to 50% at
412 Storm Peak Laboratory at an elevation of 3200 m a.s.l., in Colorado, during the time period of 28
413 April – 1 July 2008, which was suggested to be related to oxidation of upper tropospheric Hg°.
414 Overall, it is not straightforward to link directly the cause of higher RGM to lower relative
415 humidity, because in both seasons over 90% of those higher RGM samples were measured in the
416 time window of 14:00-24:00 UTC, which is the time period of lower relative humidity, stronger
417 solar radiation, and daily maximum RGM production.

418 The relationship of RGM and relative humidity at AI (marine) in spring was better
419 defined than in other seasons, and it was more scattered than that at TF (coastal), possibly
420 because of smaller variability in relative humidity in a marine environment than over land. A
421 value of 2 ppqv was used as a threshold based on the fact that the largest springtime seasonal 90^{th}
422 percentile level of RGM was 1.9 ppqv at AI (marine) (See Table 1 in Mao and Talbot, 2011),
423 and thus numbers > 2 ppqv can be considered anomalous. In springs 2008 - 2010, with
424 constraints of daytime and no precipitation, about 10% of the total 542 points showed RGM
425 mixing ratios exceeding 2 ppqv, which were observed from 14:00 – 23:59 UTC and
426 corresponded to relative humidity <70%. With the same constraints, in summers 2007, 2008,
427 and 2010 (relative humidity measurements missing in summer 2009) a total of 48 data points
428 were found with mixing ratios >2 ppqv and ~90% of them (42 out of 48) in the time window of

12:00 – 14:00 UT. Higher RGM mixing ratios were observed at all levels of relative humidity ranging from 40% - 100%. These results suggest that in the marine environment the RGM production rate in summer dominated over the dependence of loss rate on humidity yielding a rather even spread of higher levels of RGM over the spectrum of relative humidity.

There seems to be no relationship between relative humidity and Hg^P mixing ratios for all seasons at AI (marine). At TF (coastal) a correlation was observed for summers 2009 and 2010 with r^2=0.38 and 0.29 respectively and slope values of -0.006 - -0.007 ppqv Hg^P per 1% relative humidity. The reason for this relationship is unclear.

3.5 Precipitation

Effects of precipitation on RGM and Hg^P at TF (coastal) and AI (marine) were examined for all seasons. The seasonal averages ($\pm 1\sigma$) for RGM at TF (coastal) under rainy and dry conditions are summarized in Table 1. Note that precipitation data are not available at PM (inland), and thus PM (inland) is not considered. In the four summers of 2007 – 2010, the average levels of RGM under dry conditions varied from 0.1 to 0.2 ppqv, whereas more than 95% of the samples under rainy conditions were below the LOD except summer 2009. In summer 2009 a little over half of the data points from rainy conditions were below the LOD, and therefore that was the only summer with the average RGM level barely above the LOD. Similarly in all four falls the majority of RGM mixing ratios (>80%) were below the LOD under rainy conditions. In spring and winter relatively more chances were RGM mixing ratios remaining above the LOD during rainfalls. In springs of 2007 – 2010 seasonal averages under rainy conditions varied around 0.2 ppqv with less than half of the samples below the LOD and those under dry conditions were a factor of 3 – 4 to two orders of magnitude higher, suggesting that the RGM production rate dominated over the washout effect of precipitation in spring. In

452 winters of 2007 – 2010, only snowfalls were considered, and three-hourly accumulated
453 precipitation from snowfalls hardly exceeded 10 mm, none in winter 2010. In contrast to
454 summer, RGM mixing ratios appeared to be mostly above the LOD during snowfalls at
455 0.14±0.20, 0.18±0.33, 0.45±0.23, and 0.14±0.21 ppqv for the 2007 – 2010 winters, suggesting
456 less scavenging efficiency from snow compared to liquid precipitation.

457 Further examination of RGM at TF (coastal) separated the data into three subsets: days
458 without rain (i.e., dry), with nighttime rain, and with daytime rain. Diurnal cycles were averaged
459 seasonally each year for each subset (Figure 15). Five main characteristics are summarized here.
460 First, the diurnal cycle on dry days was well-defined with minimum values before sunrise and
461 peaks over 15:00 – 17:00 UTC, and the annual maximum daily amplitude (daily maximum –
462 minimum) occurred in spring varying from 0.8 ppqv in 2010 to 1.8 ppqv in 2007. Second, in
463 contrast to the dry days, the diurnal variation was dampened greatly on days with nighttime rain,
464 e.g. a daily amplitude of 0.3 ppqv in spring 2010 and 0.7 ppqv in spring 2007, and there was
465 little to no variability on days with daytime rain. In other words, even if it rained before sunrise
466 and it was dry during the daytime, the daily peak did not go back to the levels of dry days. This
467 suggests that RGM in the residual layer was washed out at night leading to less contribution to
468 the surface level of RGM via downward mixing from aloft after sunrise. Third, for springtime
469 dry days, the daytime RGM mixing ratios were the largest of all seasons and under all conditions
470 with discernible year-to-year fluctuations in the daily maximum, varying from 1 ppqv in spring
471 2010 to 2.3 ppqv in spring 2007. Fourth, for dry days the magnitude and pattern of diurnal
472 variation appeared to be similar between summer and fall, although there seemed to be larger
473 year-to-year variability in daytime RGM levels in the fall. Fifth, nighttime RGM levels in winter,
474 be it dry or wet, were lower than those in spring but higher than in summer and fall.

475 Closer examination of changes in RGM at the onset of and during rainfalls in summer
476 and spring at TF (coastal) revealed two main characteristics. First, the RGM levels generally fell
477 below the LOD immediately after a rainfall began nearly independent of the precipitation
478 amount. Second, there were 12 exceptional events, mostly in spring and summer, where RGM
479 actually increased during a rainfall, and there were four rainfalls lasting 9 – 19 hours with RGM
480 mixing ratios consistently hovering at levels above the LOD (Table 2).

481 Diurnal and seasonal variability in Hg^P at TF (coastal) appeared to be smaller than that of
482 RGM at TF (coastal) in the three subsets of data (Figure 16). On dry days, the magnitude of Hg^P
483 variability in spring was close to that in winter, with both hovering around 0.5 ppqv compared to
484 mostly below 0.5 ppqv in summer and fall. The diurnal variability and patterns on days with
485 nighttime and daytime rain did not differ from those on dry days as much as RGM, meaning Hg^P
486 was rarely washed out entirely by precipitation and most samples remained above the LOD. A
487 few sample points of Hg^P below the LOD were found during snowfalls: 1.) when a snowfall
488 started at night and lasted throughout the night, or 2.) when rain preceded the snowfall, and
489 likely reduced the Hg^P mixing ratio substantially before the snow began.

490 For AI (marine) we used 6-hourly precipitation data, which is different from the hourly
491 time resolution for TF (coastal). This is because the only available precipitation data for AI are
492 the 6-hourly data from the National Weather Service monitoring site at the Pease Airport, about
493 10 km from AI. To match that, we integrated RGM over the 6-hour interval. Without hourly
494 precipitation data it is impossible to examine in detail the effects of precipitation on RGM;
495 therefore, we can only report the general features observed in the 6-hourly averaged data. At AI
496 (marine) under dry conditions, seasonally averaged mixing ratios remained well above the LOD
497 in all seasons with remarkable year-to-year variability (Table 3). For example, in spring the

498 average was lowest in 2010 at 0.37 ppqv and highest in 2008 at 0.89 ppqv, and in fall the lowest
499 average was found to be 0.26 ppqv in 2008 and highest 0.59 ppqv in 2009.

500 Furthermore, similar to TF (coastal), under dry conditions the seasonally averaged
501 diurnal patterns of RGM at AI (marine) were better defined in spring and summer than fall and
502 winter (Figure 17). Overall nighttime and daytime precipitation dampened diurnal variability
503 lowering RGM levels throughout the day except in winter when nighttime precipitation
504 suppressed mixing ratios only during the nighttime and conversely daytime precipitation only
505 lowered the daytime mixing ratios. Summer 2007 and fall 2009 appeared to be quite different
506 with much higher mixing ratios on days with nighttime or daytime precipitation. A closer look
507 revealed that the RGM mixing ratio was only slightly decreased by precipitation events in
508 summer 2007, and in fall 2009 there were ~10 days over 21 October – 1 November when
509 particularly strong precipitation events were accompanied by unusually high levels of RGM. A
510 preliminary examination of limited chemical tracers (only CO and O_3 were available) and
511 trajectories did not suggest any particularly dominant mechanisms driving the unusual behavior
512 in RGM during those two seasons (Mao et al., 2012).

513 There were three distinct characteristics of the impacts of precipitation on Hg^P at AI
514 (marine): 1.) seasonal averaged mixing ratios hovered around the LOD under rainy conditions in
515 all seasons, 2.) highest seasonal averaged levels under dry condition occurred in fall and summer
516 and lowest in winter, and 3.) compared to RGM, there appeared to be smaller variability in
517 seasonal average levels for both rainy and dry conditions (Table 4). The three subsets of Hg^P
518 data, i.e., dry, with nighttime rain, and with daytime rain, suggested that occurrence of rain, be it
519 at night or during the day, had negligible impact on the magnitude and pattern of diurnal
520 variation of Hg^P at AI (marine) in all seasons (Figure 18). Moreover, there was little variability

521 in the four seasons under the three conditions, except in fall 2009 which was a unique case.

522 **4. Discussion**

523 As summarized in the Introduction, relationships between mercury and physical
524 parameters had been examined using limited datasets ranging from weeks to 1-2 years in
525 previous studies. The most commonly studied relationships are ones that Hg° or TGM has with
526 temperature and wind. A few studies explored how speciated mercury was related to solar
527 radiation, relative humidity and precipitation using daily or seasonal average levels of mercury
528 for such examination. To the best of our knowledge, our study is the first attempt to examine
529 aforementioned relationships using long-term continuous measurement data of highest temporal
530 resolution for different seasons and contrasting geographical environments. We found that one-
531 to-one corresponding relationships between speciated mercury and physical parameters of high
532 temporal resolution were too scattered to yield meaningful correlations except Hg° vs.
533 temperature in the coastal and inland environments during the warm season. However, subsets
534 of data disclosed better defined relationships, in large part due to the dominance of a single
535 parameter in the processes that were captured in those subsets of data. Further, tendencies of
536 speciated mercury with respect to changes of individual physical parameters were revealed when
537 their magnitude ranges were discretized into small bins. In this section key findings are
538 summarized in Table 5 and are discussed in comparison to previous works.

539 4.1 Wind

540 Effects of wind on ambient levels of speciated mercury had been demonstrated to mainly
541 facilitate transport from upwind sources by examining the wind rose of mercury concentrations
542 and backward trajectories of mercury rich air masses (e.g., Poissant et al., 2005; Gariel et al.,
543 2005; Sigler et al., 2009a; Aucott et al., 2009) and to enhance mercury evasion (Gårdfeldt et al.,

544 2003; Sigler et al., 2009b). Our study confirmed such effects of wind speed and direction on
545 mercury. In particular, we revealed a somewhat positive correlation between Hg^o and wind
546 speed with minimal anthropogenic influence indicative of oceanic origin during a major storm
547 over 14 – 16 November 2008. This effect reached TF (coastal) and PM (inland) causing
548 synchronized changes in Hg° at all three sites. This finding corroborated our hypothesis in
549 Sigler et al. (2009b) that strong wind induced enhancement in oceanic emissions of Hg° can have
550 a regional influence on ambient levels of Hg° that can reach far inland.

551 We found very few RGM mixing ratios exceeding the LOD at the inland rural elevated
552 site. At the coastal site, higher RGM levels were speculated to possibly result from local
553 production and transport. These higher levels nearly all occurred in the time window of 18:00 –
554 23:00 UTC when solar radiation was strongest. Transport of RGM to the coastal site was
555 supported by the evidence that RGM >3 ppqv occurred in two ranges, southeasterly (~135°) and
556 southerly to northwesterly (180°-315°), the flow regimes that facilitated pollutant transport from
557 sources in the Northeast (Mao and Talbot, 2004b). Moreover, these relatively high RGM levels
558 seemed to be associated with large SO_2 mixing ratios indicating combustion sources, which will
559 be further investigated in a separate manuscript on the relationships between mercury and key
560 chemical compounds (Mao et al., 2012).

561 In the marine environment RGM mixing ratios appeared to be less dependent on wind
562 speed. However a few sample points with mixing ratios >4 ppqv, which occurred in spring, were
563 mostly from the south and the west, whose upwind source regions are the greater Boston area
564 and southern NH. It is curious that RGM could survive the transport over a distance of 4-5 hours,
565 i.e., ~80 km, in the marine air laden with sea salt aerosols. It implies strong net production of
566 RGM in transit, largely in the marine environment in addition to possible anthropogenic

567 contributions. Further, it could also result from release of RGM in the form of $HgCl_2$ from the
568 surface of sea salt aerosols as suggested by Pirrone et al. (2000) and the several days of lifetime
569 of sea salt aerosols.

570 The relationship between Hg^P and wind speed differed in the coastal and marine
571 environment. While no apparent dependence of Hg^P on wind speed was observed at the coastal
572 site, a decreasing tendency in Hg^P mixing ratios with increasing wind speed at AI (marine)
573 suggested a strong impact of dry depositional loss of aerosols on ambient mixing ratios in the
574 marine environment. Mixing ratios of Hg^p over the range of 0.5 – 1.5 ppqv concurrent often with
575 westerly flow indicates a land influence on the marine site.

576 4.2 Solar radiation

577 Consistent with previous studies, positive relationships were observed between solar
578 radiation and RGM as well as Hg^P in coastal and marine environments in the warm season.
579 Furthermore, our results suggested seasonal difference between sites for RGM. A positive
580 relationship between RGM and solar radiation was found in spring in the coastal environment,
581 while in both spring and summer at the marine site. Additionally the increase with radiation flux
582 was more significant at the coastal compared to the marine site.

583 Such seasonal difference indicates that the solar radiation driven production processes
584 controlling the ambient level of RGM were predominant in different seasons in the two
585 environments. In the marine boundary layer, the positive effect of solar radiation on both RGM
586 and Hg^P appeared to be dominant in the 12:00 - 18:00 UTC time quadrant, and was reduced by
587 removal processes in the 18:00 – 00:00 UTC time quadrant. This is consistent with the monthly
588 averaged diurnal variation of RGM where the mixing ratio exhibited a steady increase over 12-
589 15 UTC and leveled off after that as rates of loss and production became comparable.

590 Also, compared to the coastal environment more factors can affect RGM production in
591 the marine environment in addition to solar radiation, including halogen radical concentrations
592 and sea salt aerosol concentrations. The seasonal and diurnal variabilities in these factors may
593 not be synchronized and thus different combinations of factors may weigh in on their influences
594 on RGM production at different times. Halogen radical concentrations are dependent on solar
595 radiation, which is indirectly supported by observed halocarbons reaching annual minimum in
596 summer due to faster photodissociation (Zhou et al., 2008) conducive to higher levels of halogen
597 radical concentrations. This may explain why the effect of solar radiation on RGM was observed
598 in both spring and summer at the marine site.

599 4.3 Temperature

600 A consistent positive, albeit not strong, correlation between Hg^o and temperature was
601 observed in spring at a remote rural location situated above the boundary layer half of the time
602 and in summer at a sea level coastal site. No such correlation was found at a site in the marine
603 boundary layer. Our previous study found significant correlation between Hg^o and temperature
604 averaged at each hour of a day over the seasons of spring and fall 2007 at TF (coastal) and AI
605 (marine) (Sigler et al., 2009a), and speculated that higher Hg^o may be attributed to thermally
606 and/or photochemically mediated release from soil (e.g., Poissant and Casimir, 1998; Sigler and
607 Lee, 2006). No consistent Hg^o-temperature correlation in the marine boundary layer during the
608 warm season seems to support this speculation.

609 Higher levels of RGM was observed at warmer temperatures during the warm season (i.e.,
610 spring and summer) and this tendency was enhanced equally for daytime data in the coastal,
611 marine, and inland environments. Lesser scavenging in winter possibly led to detectable 75^{th}
612 percentile values at the inland site. Since the diurnal and seasonal cycles of temperature and

613 solar radiation are intricately associated, it is impossible to ascertain whether and how much of
614 increasing RGM levels could be attributed to temperature and/or solar radiation separately.

615 The inland site is situated above the boundary layer, i.e., in the free troposphere, half of
616 the time and hundreds of kilometers downwind of major source regions, measurements from this
617 site capture variability in RGM in the free troposphere over rural areas. The seasonal variability
618 at that site suggests that in the midlatitude free troposphere without direct influence of major
619 anthropogenic sources: 1.) RGM mixing ratios were mostly below the LOD, 2.) the mixing ratios
620 exceeding the LOD exhibited a tendency of higher levels at warmer temperature.

621 There has been limited research on relationships between Hg^P and temperature. Our data
622 showed two opposite regimes in the Hg^P-temperature relationship: negative and positive
623 correlation at temperatures below and above 8 ^oC, respectively, corresponded to the cold and
624 warm seasons. At AI (marine) perhaps because of the missing wintertime data, there is only one
625 pattern showing values increased with warming temperature.

626 The positive relationship between Hg^P and temperature in warmer seasons possibly
627 reflects the effect of solar radiation on Hg cycling, i.e., stronger solar radiation conducive to
628 more radicals with subsequent impact on Hg° oxidation leading to more RGM and subsequently
629 more Hg^P in the coastal and marine environments. Needless to say the effect of solar radiation
630 on the surface air temperature is a direct one, too, and thus it is logical to hypothesize that the
631 positive correlation between temperature and speciated Hg (i.e., RGM and Hg^P) is more of an
632 indication of common physical mechanisms that drive variation in them than a direct link. This
633 hypothesis is in fact supported by the relationships between RGM/Hg^P and radiation flux under
634 no precipitation conditions at the coastal site as well as between RGM (Hg^P) and jNO_2 at the
635 marine site as described in Section 3.

636 4.4 Relative Humidity

637 No overall well-defined relationships were observed between Hg^o and relative humidity
638 in all three environments for all seasons. A decreasing tendency in RGM with increasing relative
639 humidity levels in all seasons was observed at the coastal site as well as the median level of
640 exceeding the LOD at the inland site in spring and winter at relative humidity <60%. It is not
641 straightforward to link directly the cause of higher RGM to lower relative humidity, because
642 over 90% of those higher RGM samples were measured in the time window of 14:00-24:00 UTC,
643 which is the time period of lower relative humidity, stronger solar radiation, and daily maximum
644 RGM production.

645 Compared to the coastal and inland sites, there was less variability in RGM with varying
646 relative humidity in the marine environment, possibly because of smaller range of relative
647 humidity and a larger production rate of RGM involving halogen chemistry which could
648 dominate over the dependence of loss rate on humidity.

649 4.5 Precipitation

650 A few studies suggested the overall scavenging effect of precipitation on RGM (Yatavelli
651 et al., 2006; Laurier et al., 2007), but none examined the dependence of the scavenging effect on
652 precipitation amount and the impact of precipitation on diurnal variability of speciated mercury
653 in different environments. Consistent with previous work, we also observed that RGM levels
654 dropped immediately below the LOD in rainfalls events independent of the precipitation amount
655 in many cases, while in some cases, mostly in spring and summer, RGM mixing ratios remained
656 above the LOD and even increased during precipitation events. In the latter cases, source
657 strengths (e.g., in situ production and transport) most likely overpowered removal of RGM. This
658 is different from the findings of Yatavelli et al. (2006) and Laurier et al. (2007) who observed

659 that RGM was invariably washed out by precipitation in the continental and marine boundary
660 layers.

661 It was also found that in winter less scavenging efficiency from snow compared to liquid
662 precipitation. This is consistent with the findings of Lombard et al. (2011) in that both the total
663 seasonal Hg wet deposition and volume-weighted Hg concentration in rain water reached the
664 annual minimum in winter during their three year sample collection at TF (coastal).

665 Our study suggested small impact of precipitation on Hg^P levels in the coastal and marine
666 environments. Talbot et al. (2011) using bulk filters for measuring Hg^P suggested a seasonal
667 shift in the aerosol size distribution. Specifically, we found that ~90% of the Hg^P was contained
668 in aerosols with aerodynamic diameters >2 micrometer (μm) at AI (marine) and TF (coastal) in
669 summer, in winter it shifted almost entirely to the fine fraction (<1 μm) below 0.5 μm with little
670 detectable in the coarse sizes, and in spring, there was a mixture of fine and coarse fractions. In
671 the same study we also suggested that the Tekran unit may not measure all the Hg^P on the coarse
672 fractions by comparing the Tekran and bulk filter measurements. Such seasonal shift in the
673 aerosol size distribution and possible limitations of Tekran 1135 measurements of Hg^P may have
674 contributed to what we have shown here. Therefore, investigation of the efficacy of Tekran 1135
675 is warranted before we can further study the causes for the observed seasonal difference in the
676 effect of precipitation or any other climate variables on Hg^P.

677 **5. Summary**

678 In this study, we present a comprehensive analysis of relationships that Hg°, RGM, and
679 Hg^P bore with climate variables in inland elevated rural, coastal, and marine environments using
680 3 – 7 years of continuous data sets of high temporal resolution. This extensive analysis of long
681 term measurement data suggested great complexity in the climate impact on ambient levels of

682 speciated mercury. More specifically, there did not appear to be simple and direct linkage
683 between Hg°/RGM/Hg^p and any physical variables; positive or negative effects were indicated
684 by the trends in Hg°/RGM/Hg^p mixing ratios corresponding to varying climatic conditions. A
685 few key points on such trends are summarized as follows.

686 • The impact of wind speed on ambient mixing ratios of Hg° in all three environments
687 was best captured during an occurrence of a strong cyclonic system in November
688 2008 when winds exceeded 15 m s^{-1} at AI (marine), in agreement with our case study
689 of the April 2007 Nor'easter in Sigler et al. (2009b). The RGM and Hg^P median, 75^{th},
690 and 90^{th} percentile values decreased with increasing wind speed in the marine
691 environment indicating enhanced loss through deposition associated with strong
692 winds in the marine boundary layer. At the coastal site RGM mixing ratios were
693 lowest under calm conditions (wind speed < 1m s^{-1}) and highest at southerly and
694 southeasterly winds >2 m s^{-1} suggesting that transport was the primary source of
695 RGM to our study location.

696 • All metrics in RGM and Hg^P appeared to increase with stronger solar radiation at the
697 coastal and marine sites.

698 • The best point-to-point correlation was found between Hg^o and temperature in
699 summer at the coastal location and spring at the inland elevated rural site. No
700 correlation was found in the marine boundary layer. This supports the speculation
701 from our previous study on thermally and/or photochemically mediated release of
702 Hg° from soil. RGM and Hg^P at all sites were positively correlated with temperature
703 in spring, summer, and fall.

704 • Relationships between RGM and relative humidity in the coastal area suggested a

clear decreasing tendency in all metrics, including 10^{th}, 25^{th}, median, 75^{th}, and 90^{th} percentile values, from less than 40% to 100% relative humidity levels in all seasons especially in spring. No relationship between relative humidity and Hg^P mixing ratios was observed for all seasons in the marine boundary layer, whereas at the coastal location correlation was observed for summers.

- The effect of precipitation on RGM at the coastal and marine locations was similar. RGM levels remained around 0.2 ppqv under rainy conditions and a factor of 3-4 to two orders of magnitude higher under dry conditions in spring. In winter RGM mixing ratios appeared to be mostly above LOD during snowfalls at 0.14±0.20, 0.18±0.33, 0.45±0.23, and 0.14±0.21 ppqv for the 2007-2010 winters at TF (coastal), suggesting less scavenging efficiency of snow. Hg^P did not seem to be washed out entirely by precipitation as RGM would be most of the time; most samples remained above the LOD. Precipitation had negligible impact on the magnitude and pattern of diurnal variation of Hg^P at the marine site AI (marine) in all seasons.

Many questions from this study remain to be addressed, e.g., quantifying strong wind induced oceanic evasion, mechanisms driving the positive correlations between mercury and temperature/solar radiation, and less impact of relative humidity and precipitation on Hg^P than on RGM. In addition, longer continuous measurement data of Hg°, RGM, and Hg^P are imperative to obtain rigorous quantification of their relationships with climate variables. Future research is warranted to obtain in-depth knowledge of the mechanisms driving those relationships.

Acknowledgements:

Funding for this work is provided by the National Science Foundation under grant# ATM1141713, the National Oceanic and Atmospheric Administration AIRMAP program under

728 grant# NA07OAR4600514, and the Environmental Protection Agency under contract
729 #EP09H000355. We thank Cheryl Parker and Kevan Carpenter for their technical assistance.
730 We thank J Sigler for his work on initiating and maintaining RGM measurement at AIRMAP
731 sites.
732

References:

Aucott, M. L., A. D. Caldarelli, R. R. Zsolway, C. B. Pietarinen, and R. England (2009), Ambient elemental, reactive gaseous, and particle-bound mercury concentrations in New Jersey, U.S.: measurements and association with wind direction, *Environ. Monit. Assess., 158*, 295-306.

Baya, A. P., and B. van Heyst (2010), Assessing the trends and effects of environmental parameters on the behavior of mercury in the lower atmosphere over cropped land over four seasons, *Atmos. Chem. Phys., 10*, 8617-8628.

Brooks, S., W. Luke, M. Cohen, P. Kelly, B. Lefer, B. Rappenglück (2010), Mercury species measured atop the Moody Tower TRAMP site, Houston, Texas, *Atmos. Envrion.,* 44, 4045–4055.

Castillo, A. J. Valdes, J. Sibaja, I. Vega, R. Alfaro, J. Morales, G. Esquivel, E. Barrantes, P. Black, and D. Lean (2011), Seasonal and diel patterns of total gaseous mercury concentration in the atmosphere of the Central Valley of Costa Rica, *Appl. Geochem., 26,* 242-248.

Cobbetta, F. D., A. Steffen, G. Lawson, B. J. Van Heyst: GEM fluxes and atmospheric mercury concentrations (GEM, RGM and Hg^P) in the Canadian Arctic at Alert, Nunavut, Canada (February – June 2005), *Atmos. Environ., 41*, 6527 – 6543, 2007.

Cole, A. S., and A. Steffen (2010), Trends in long-term gaseous mercury observations in the Arctic and effects of temperature and other atmospheric conditions, *Atmos. Chem. Phys., 10,* 4661-4672.

754 Faïn, X., Obrist, D., Hallar, A. G., Mccubbin, I., and Rahn, T.: High levels of reactive gaseous
755 mercury observed at a high elevation research laboratory in the Rocky Mountains,
756 Atmos. Chem. Phys., 9, 8049–8060, 2009.
757 Feddersen, D., R. Talbot, H. Mao (2011), Size distribution of particulate mercury in marine and
758 continental atmospheres, *Atmosphere*, in preparation.
759 Gårdfeldt, K., J. Sommar, R. Ferrara, C. Ceccarini, E. Lanzilotta, J. Munthe, I. Wangberg, O.
760 Lindqvist, N. Pirrone, P. Sprovieri, E. Pesenti (2003): Evasion of mercury from Atlantic
761 coastal water and the Mediterranean sea, coastal and open water, *Atmos. Environ., 37*,
762 Suppl. 1, 73-84.
763 Gabriel, M. C., D. G. Williamson, S. Brooks, and S. Lindberg (2005), Atmospheric speciation of
764 mercury in two contrasting Southeastern US airsheds, *Atmos. Environ., 39*, 4947-4958.
765 Han, Y.-J., T. M. Holsen, S.-O. Lai, Hopke, P. K., Yi, S.-M., Liu, W., Pagano, J., Falanga,
766 L., Milligan, M., Andolina, C. (2004), Atmospheric gaseous mercury concentrations in
767 New York State: relationships with meteorological data and other pollutants, *Atmos.*
768 *Environ., 38*, 6431-6446.
769 Jacob, D., and D. A. Winner (2009), Effect of climate change on air quality, *Atmos. Environ.*, *43,*
770 51–63.
771 Kim, S. Y., Talbot, R., Mao, H.: Cycling of Gaseous Elemental Mercury: Importance of Water
772 Vapor, submitted to *Geophys. Res. Lett.*, 2011.
773 Kock, H. H., E. Bieber, R. Ebinghaus, T.G. Spain, B. Thees (2005), Comparison of long-term
774 trends and seasonal variations of atmospheric mercury concentrations at the two
775 European coastal monitoring stations Mace Head, Ireland, and Zingst, Germany, *Atmos.*
776 *Environ., 39*, 7549 – 7556.

777 Laurier, F. J. G., Mason, R. P., and Whalin, L.: Reactive gaseous mercury formation in the
778 North Pacific Ocean's marine boundary layer: A potential role of halogen chemistry, J.
779 Geophys. Res., 108 (D17), 4529, doi:10.1029/2003JD003625, 2003.
780 Laurier, F., and Mason, R.: Mercury concentration and speciation in the coastal and open ocean
781 boundary layer, *J. Geophys. Res., 112*, D06302, doi:10.1029/2006JD007320, 2007.
782 Li, Z., C. Xia, X. Wang, Y. Xiang, and Z. Xie (2011), Total gaseous mercury in Pearl River
783 Delta region, China during 2008 winter period, *Atmos. Environ., 45*, 834-838.
784 Liu, B., Keeler, G. J., Dvonch, , J. T, Barres, J. A., Lynam, M. M., Marsik, F. J., Morgan, J. T.,
785 Temporal variability of mercury speciation in urban air, *Atmos. Environ., 41*, 1911-1923,
786 2007.
787 Lombard, M. A. S., J. Bryce, H. Mao, and R. Talbot (2011), Mercury wet deposition in southern
788 New Hampshire, 2006 - 2009, *Atmospheric Chemistry and Physics Discuss., 11*, 4569 -
789 4598.
790 Mao, H., and R. Talbot (2004a), O_3 and CO in New England: Temporal variations and
791 relationships*, J. Geophys. Res*., *109*, D21304, doi:10.1029/2004JD004913.
792 Mao, H. and R. Talbot (2004b), The role of meteorological processes in two New England ozone
793 episodes during summer 2001, *J. Geophys. Res*., *109,* (D20305),
794 doi:10.1029/2004JD004850.
795 Mao, H., R. Talbot, J. M. Sigler, B. C. Sive, and J. D. Hegarty (2008), Seasonal and diurnal
796 variation in Hg° over New England, *Atmos. Chem. Phys., 8*, 1403-1421.
797 Mao, H., and R. Talbot (2011), Speciated Mercury at Marine, Coastal, and Inland Sites in New
798 England: Part I. Temporal Variability, *Atmos. Chem. Phys. Discuss., 11,* 32301–32336.

799 Mao, H., and R. Talbot, et al. (2012), Speciated Mercury at Marine, Coastal, and Inland Sites in
800 New England: Part III. Relationships with Key Trace Gases, to be submitted to *Atmos.*
801 *Chem. Phys.*
802 Mason, R. P., and G.-R. Sheu (2002), Role of the ocean in the global mercury cycle, *Global Bio.*
803 *Cycles, 16*(4), 1093, doi:10.1029/2001GB001440.
804 Obrist, D., Tas, E., Peleg, M., Matveev, V., Faïn, X., Asaf, D., and Luria, M.: Bromine-induced
805 oxidation of mercury in the mid-latitude atmosphere, *Nature Geosci., 4*, 22-26, DOI:
806 10.1038/NGEO1018, 2011.
807 Pacyna, E. G., Pacyna, J. M., Steenhuisen, F., Wilson, S.: Global anthropogenic mercury
808 emission inventory for 2000, *Atmos. Environ., 40 (22)*, 4048,
809 doi:10.1016/j.atmosenv.2006.03.041, 2006.
810 Pirrone, N., Hedgecock, I.M., Forlano, L.: The role of the ambient aerosol in the atmospheric
811 processingof semivolatile contaminants: A parameterised numerical model (gaspar), J.
812 Geophys. Res., 105 (D8), 9773 – 9790.
813 Poissant, L., M. Pilote, X. Xu, H. Zhang, and C. Beauvais (2004), Atmospheric mercury
814 speciation and deposition in the Bay St. François wetlands, *J. Geophys. Res., 109*,
815 D11301, doi:1029/2003JD004364.
816 Poissant, L., Pilote, M., Xu, X., Beauvais, C., Constant, P., and Zhang, H. (2005), A year of
817 continuous measurements of three atmospheric mercury species in southern Quebec,
818 Canada, Atmos. Environ., 39, 1275–1287.
819 Sigler, J. M., H. Mao, and R. Talbot (2009a), Gaseous elemental and reactive mercury in
820 southern New Hampshire, *Atmos. Chem. Phys.*, 9, 1929-1942.

821 Sigler, J. M., H. Mao, B. Sive, and R. Talbot (2009b), Oceanic Influence on Atmospheric
822 Mercury at Coastal and Inland Sites: A Springtime Nor'easter in New England, *Atmos.*
823 *Chem. Phys., 9*, 4023-4030.
824 Sprovieri, F., N. Pirrone, R. Ebinhaus, H. Kock, and A. Dommergue, Worldwide atmophseric
825 mercury measurements: a review and synthesis of spatial and temporal trends, Atmos.
826 Chem. Phys. Discuss., 10, 1261-1307, 2010.
827 Stamenkovic, J., S. Lyman, M. S. Gustin: Seasonal and diel variation of atmospheric mercury
828 concentrations in the Reno (Nevada, USA) airshed, *Atmos. Environ., 41*, 6662 – 6672,
829 2007.
830 Talbot R., H. Mao, and B. Sive (2005), Diurnal characteristics of surface-level O_3 and other
831 important trace gases in New England, *J. Geophys. Res.*, 110, D09307,
832 doi:10.1029/2004JD005449.
833 Talbot, R., H. Mao, D. Feddersen, M. Smith, S. Y. Kim, B. Sive, K. Haase, J. Ambrose, Y. Zhou
834 and R. Russo (2011), Comparison of particulate mercury measured with manual and
835 automated methods, *Atmosphere 2*(1), 1-20; doi:10.3390/atmos2010001.
836 Yatavelli, R. L. N., Fahrni, J. K., Kim, M., Crist, K. C., Vickers, C. D., Winter, S. E., and
837 Connell, D. P.: Mercury, PM2.5 and gaseous co-pollutants in the Ohio River Valley
838 region: Preliminary results from the Athens supersite, Atmos. Environ., 40, 6650–6665,
839 2006.
840 Zhou, Y., H. Mao, R. S. Russo, D. R. Blake, O. W. Wingenter, K. B. Haase, R. K. Varner, R.
841 Talbot, and B. C. Sive (2008), Bromoform and dibromomethane measurements in the
842 seacoast region of New Hampshire, 2002-2004, *J. Geophys. Res.*, 113, D08305,
843 doi:10.1029/2007JD009103.

Table 1. Seasonal mean (denoted as avg) ± 1σ values (ppqv) of RGM at Thompson Farm for rainy and dry conditions. N stands for the number of samples. N_b stands for the number of samples with RGM below the LOD.

	Rainy			dry	
	N	N_b	Avg±1σ	N	Avg±1σ
Spring 2007	118	59	0.19±0.32	900	0.99±1.68
2008	111	48	0.19±0.25	905	0.59±1.18
2009	95	34	0.26±0.23	562	0.75±0.90
2010	94	56	0.01±0.18	506	0.38±0.56
Summer 2007	71	69	0.01±0.03	1020	0.21±0.50
2008	85	81	0.02±0.05	894	0.11±0.33
2009	106	58	0.11±0.09	580	0.20±0.36
2010	58	56	0.03±0.03	651	0.21±0.36
Fall 2006	47	44	0.03±0.05	229	0.16±0.39
2007	93	77	0.07±0.15	935	0.25±0.59
2008	99	88	0.03±0.06	748	0.09±0.23
2009	48	33	0.11±0.12	431	0.13±0.16
Winter 2007	79	45	0.14±0.20	947	0.37±0.50
2008	164	90	0.18±0.32	863	0.22±0.42
2009	20	0	0.46±0.23	200	0.53±0.39
2010	58	34	0.14±0.21	402	0.14±0.19

Table 2. At TF (coastal) Rainfalls during which RGM levels (ppqv) were not washed out maintaining above the LOD together with precipitation amount (mm) for each sample cycle. The rainfall episodes on the left saw increasing RGM levels, and the ones on the right (shaded) had sustained RGM levels during rainfalls that lasted hours.

	RGM	Rain
3/15/2007 12:23:00	0.11	0.3
3/15/2007 14:23:00	0.25	0.8
3/15/2007 16:23:00	0.31	0.9
4/13/2007 00:18:00	0.00	4.5
4/13/2007 02:18:00	0.08	3.9
4/13/2007 04:18:00	0.29	0.4
4/15/2007 14:48:00	0.44	0.7
4/15/2007 16:48:00	0.38	5.7
4/15/2007 18:48:00	0.56	5.1
4/15/2007 20:48:00	0.42	4.4
4/15/2007 22:48:00	0.57	5.6
2/28/2008 05:37:00	0.00	0.6
2/28/2008 07:37:00	1.09	0.3
3/12/2008 17:27:00	0.14	1.5
3/12/2008 19:27:00	0.49	0.2
3/19/2008 06:02:00	0.19	0.2
3/19/2008 08:02:00	0.61	0.4
4/28/2008 20:32:00	0.13	8.8
4/28/2008 22:32:00	0.53	7.7
10/22/2008 01:52:00	0.04	0.6
10/22/2008 03:52:00	0.26	0.2
2/20/2009 03:01:00	0.47	0.9
2/20/2009 05:56:00	0.51	6.0
2/20/2009 08:51:00	1.14	1.4
5/7/2009 07:41:00	0.54	6.5
5/7/2009 10:36:00	0.54	10.2
5/7/2009 13:31:00	0.32	3.5
5/7/2009 16:26:00	0.28	0.3
10/7/2009 09:22:00	0.27	2.8
10/7/2009 17:22:00	0.63	1.1
10/7/2009 20:22:00	0.44	0.4
10/25/2009 04:52:00	0.24	3.1
10/25/2009 07:52:00	0.22	0.7

	RGM	Rain
4/4/2007 23:22:00	0.25	4.2
2/19/2009 14:01:00	0.22	5.0
6/19/2009 00:51:00	0.34	2.2
6/19/2009 03:46:00	0.28	4.8
6/19/2009 06:41:00	0.30	9.6
6/19/2009 10:16:00	0.31	5.3
6/19/2009 13:11:00	0.31	1.7
6/19/2009 16:06:00	0.34	7.7
6/19/2009 19:01:00	0.32	2.1
6/21/2009 12:31:00	0.21	0.4
6/21/2009 15:26:00	0.20	0.5
6/21/2009 18:21:00	0.25	1.0
7/2/2009 09:26:00	0.21	0.4
7/2/2009 12:21:00	0.21	2.6
7/2/2009 15:16:00	0.21	15.9
7/2/2009 18:11:00	0.26	2.1
7/2/2009 21:06:00	0.22	6.0
7/3/2009 00:01:00	0.22	1.5
11/20/2009 11:22:00	0.27	0.5
3/13/2010 23:47:00	0.17	1.7
3/14/2010 03:22:00	0.20	3.9
3/14/2010 06:22:00	0.22	12.2
4/16/2010 12:27:00	0.26	0.4
4/16/2010 15:27:00	0.25	1.2
4/16/2010 18:27:00	0.33	1.7
4/16/2010 21:27:00	0.38	3.8
4/17/2010 00:27:00	0.26	1.1

Table 3. Seasonal mean (denoted as avg) ± 1σ values (ppqv) of RGM at Appledore Island for rainy and dry conditions. N stands for the number of samples.

	Rainy		dry	
	N	Avg±1σ	N	Avg±1σ
Spring 2008	57	0.30±0.36	386	0.89±1.22
2009	70	0.09±0.19	537	0.69±1.03
2010	62	0.05±0.11	463	0.37±0.65
Summer 2007	36	0.59±0.40	476	0.83±0.79
2008	64	0.17±0.23	544	0.47±0.66
2009	79	0.09±0.42	276	0.37±0.47
2010	38	0.22±0.53	562	0.60±1.02
Fall 2006	57	0.02±0.02	133	0.46±0.46
2008	59	0.08±0.14	236	0.26±0.36
2009	52	0.33±0.70	255	0.59±0.98
Winter 2009	65	0.17±0.13	293	0.50±0.40
2010	62	0.01±0.03	185	0.07±0.31

Table 4. Seasonal mean (denoted as avg) ± 1σ values (ppqv) of Hg^P at Appledore Island for rainy and dry conditions. N stands for the number of samples.

	Rainy		dry	
	N	Avg±1σ	N	Avg±1σ
Spring 2009	52	0.08±0.13	257	0.27±0.21
2010	62	0.11±0.19	495	0.37±0.52
Summer 2009	79	0.09±0.13	426	0.43±0.38
2010	38	0.35±0.28	625	0.58±0.36
Fall 2009	52	0.36±0.72	364	0.54±2.10
Winter 2009	65	0.08±0.07	193	0.13±0.16

Table 5. Summary of key results in the coastal, marine, and inland environments.

		Coastal (TF)	Marine (AI)	Inland elevated rural (PM)
Wind	Hg°	Transport and oceanic evasion	Transport and oceanic evasion	Transport and oceanic evasion
	RGM	Transport and local production	No dependence except values >4 ppqv corresponding to wind from the south and west indicative of transport from upwind Boston and southern NH	The very few points >LOD associated with upwind coal-fired power plants
	Hg^P	No apparent dependence	A decreasing tendency with increasing wind speed Values of 0.5 - 1.5 ppqv corresponding to westerly wind	-- (no Hg^P data)
Solar Radiation	Hg°	No relation	No relation	-- (no radiation data)
	RGM	Positive tendency in spring	Positive tendency in spring and summer	--
	Hg^P	Positive tendency in summer	Positive tendency in summer except that Hg^P turned downward at $jNO_2 > 0.008\ s^{-1}$	--
Tempera-ture	Hg°	Positive correlation with fairly consistent r^2 and slope values	No correlation	Positive correlation with fairly consistent r^2 and slope values
	RGM	Higher levels of RGM was observed at warmer temperatures during the warm season	RGM >LOD at warmer temperatures during the warm season Detectable 75th percentile values in winter	Higher levels of RGM was observed at warmer temperatures during the warm season
	Hg^P	Two opposite regimes: negative and positive correlation at temperatures below and above 8ºC, respectively	Possibly due to missing winter data, only one pattern showing increasing mixing ratios with warming temperature	--

Table 5. Continued

		Coastal (TF)	Marine (AI)	Inland elevated rural (PM)
Relative Humidity	Hg°	No overall well-defined relationship	No overall well-defined relationship; August data showed a linear correlation forming the upper boundary of its relationship	No overall well-defined relationship
	RGM	Decreasing tendency in all seasons	Less variability over all bins of relative humidity; the highest levels in summer for relative humidity <50%	In spring and winter for relative humidity below 60% the median level of RGM exceeded the LOD
	Hg^P	Correlation in summers 2009 and 2010 with r^2=0.38 and 0.29 respectively and slope values of -0.006 - -0.007 ppqv Hg^P per 1% relative humidity	No relationship for all seasons	--
Precipi-tation	Hg°	No relation	No relation	No relation
	RGM	In summer 95% of the samples under rainy conditions below the LOD and 80% in fall. In spring and winter relatively more RGM mixing ratios above the LOD during precipitation events. RGM mixing ratios mostly above the LOD during snowfalls. Diurnal variation dampened greatly on days with nighttime rain, and little to no variability on days with daytime rain.	Nighttime and daytime precipitation dampened diurnal variability lowering RGM levels throughout the day in the warm season. In winter nighttime precipitation suppressed mixing ratios during the nighttime only and conversely daytime precipitation lowered the daytime mixing ratios only.	--

Table 5. Continued.

		Coastal (TF)	Marine (AI)	Inland elevated rural (PM)
		RGM levels falling below the LOD immediately after a rainfall began nearly independent of the precipitation amount. Twelve events with RGM increasing during a rainfall four rainfalls lasting 9 – 19 hours with RGM mixing ratios consistently hovering at levels above the LOD		
	Hg^P	Diurnal variability and patterns on days with night- and daytime rain did not differ from those on dry days as much as RGM	Negligible impact on the magnitude and pattern of diurnal variation of Hg^P at AI (marine) in all seasons	--

Figure captions:

Figure 1. (a) Wind speed (blue dots) and direction (solid black circles), mixing ratios of Hg° (dark grey) and CO (light grey) at AI (marine) during 20 October – 30 November 2008, (b) a zoom-in on 13 – 17 November 2008 and (c) the Hg^{o}-wind speed correlation with r^2=0.18, slope = 3.7 ppqv per 1 m s^{-1} for the zoom-in period.

Figure 2. Surface analysis from the Hydrometeorological Prediction Center (http://www.hpc.ncep.noaa.gov/) for 0000 UTC November 16, 2008. Sea level pressure is contoured with reddish brown lines every 4 hPa. Cold (blue), warm (red), and occluded (purple) frontal positions are also shown and central pressures (hPa) of highs and lows are shown with underlined numbers.

Figure 3. Hg^{o} mixing ratios at TF (coastal) (a) and PM (inland) (b) during the time period of 1 – 17 November 2008.

Figure 4. RGM mixing ratios versus wind speed and direction at TF (coastal) (a,b), AI (marine) (c,d), and PM (inland) (e,f).

Figure 5. Hg^{P} mixing ratios versus wind speed and wind direction at TF (coastal) (a,b) and AI (marine) (c,d)

Figure 6. a) RGM versus surface solar radiation flux at TF (coastal) in spring, b) RGM versus jNO_2 at AI (marine) in spring and summer, c) Hg^{P} versus surface solar radiation flux at TF (coastal) in summer, and d) Hg^{P} versus jNO_2 at AI (marine) in summer. Only daytime data were used.

Figure 7. Mixing ratios of Hg^{o} versus temperature in summers of 2004 – 2010 at TF (coastal). The lines indicate the 95% confidence interval.

Figure 8. Mixing ratios of Hg^o versus temperature in springs 2007 – 2010 at PM (inland). The lines indicate the 95% confidence interval.

Figure 9. Daytime mixing ratios of RGM versus temperature at TF (coastal) in (a) springs and (b) summers 2003 – 2010, at AI (marine) in (c) springs, (d) summers, and (e) winters 2007 – 2010.

Figure 10. Relationships between Hg^P and temperature at TF (coastal) for (a) all seasons, (b) daytime springs, (c) daytime summers, and (d) winters during January 2009 – August 2010.

Figure 11. Relationships between Hg^P and temperature at AI (marine) for (a) all seasons, (b) springs, (c) summers, and (d) falls during April 2009 – August 2010. There was only one month data for the winter season during the entire study period.

Figure 12. Relationships between Hg^o and relative humidity at AI (marine) for summers (a) 2007, (b) 2008, and (c) 2010. Points forming the linear upper boundary are highlighted in red. Relationships between Hg^o and temperature (d,e), temperature and relative humidity (f,g) for the points in the upper boundary in summers 2008 and 2010.

Figure 13. Relationships between RGM and relative humidity at TF (coastal) (a-e) and AI (marine) (f-j) for all seasons (a,f), springs (b,g), summers (c,h), falls (d,i), and winters (e,j).

Figure 14. Relationships between RGM and relative humidity at TF (coastal) in (a) springs, (b) summers, (c) falls, and (d) winters with data from 2007 in black, 2008 in red, 2009 in green and 2010 in blue.

Figure 15. Diurnal cycles of RGM at TF (coastal) averaged over days without rain (a), days with nighttime rain (b), and days with daytime rain (c) for all seasons during 2006 – 2010. It should be noted that there were data in February only in winter 2009 and there were too few data for conditions in (b) and (c) in winter to be presented for comparison. Similarly there were data in November only for fall 2006 and there were insufficient data in Fall 2006 for (b). Precipitation in winter includes rain and snow.

Figure 16. Diurnal cycles of Hg^P at TF (coastal) averaged over days without rain (a), days with nighttime rain (b), and days with daytime rain (c) for all seasons during 2009 – 2010. Precipitation in winter includes rain and snow.

Figure 17. Diurnal cycles of RGM at AI (marine) averaged over days without rain (a), days with nighttime rain (b), and days with daytime rain (c) for all seasons during 2007 – 2010. Precipitation in winter includes rain and snow.

Figure 18. Diurnal cycles of Hg^P at AI (marine) averaged over days without rain (a), days with nighttime rain (b), and days with daytime rain (c) for all seasons during 2009 – 2010. Precipitation in winter includes rain and snow.

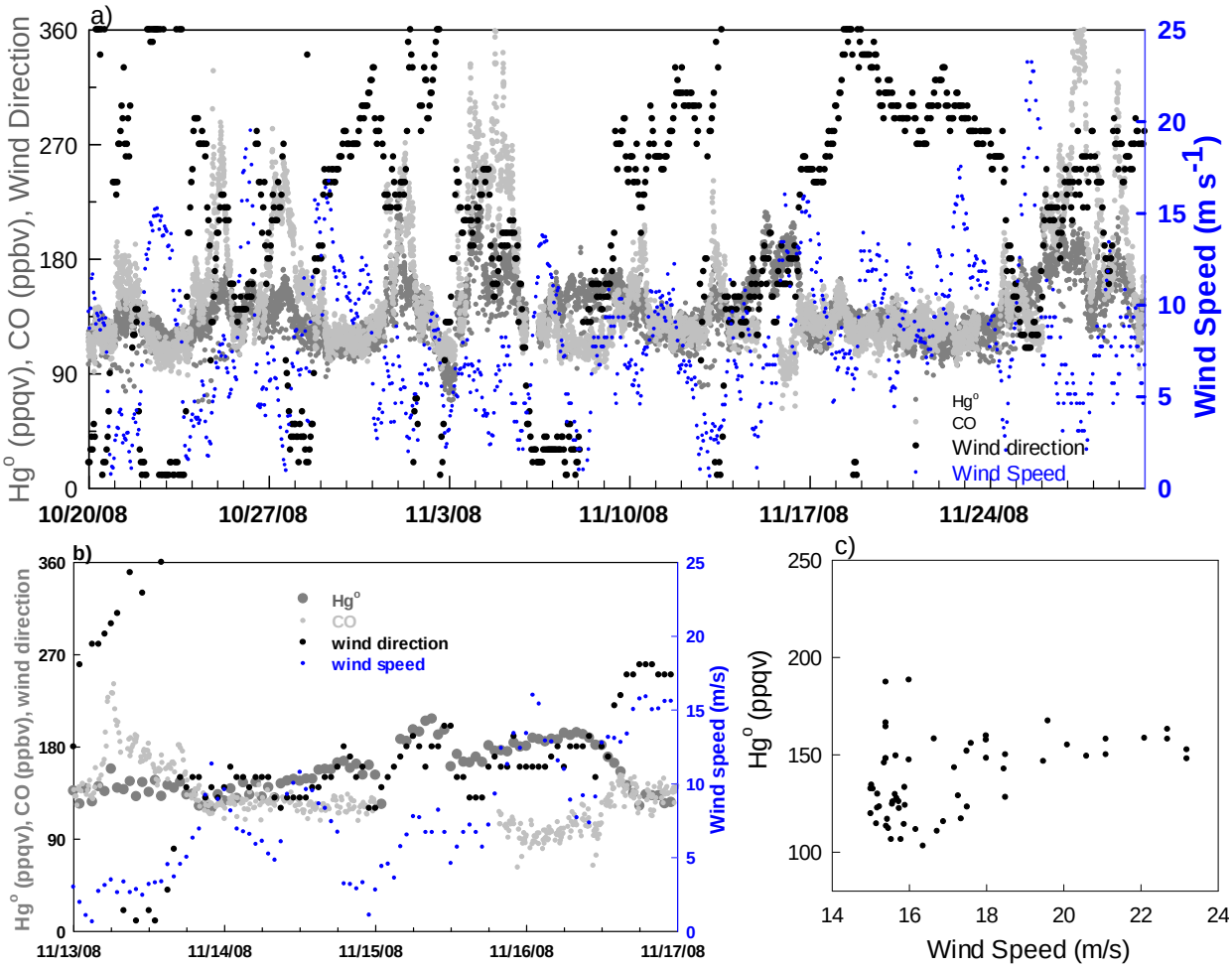

Figure 1. (a) Wind speed (blue dots) and direction (solid black circles), mixing ratios of Hg° (dark grey) and CO (light grey) at AI (marine) during 20 October – 30 November 2008, (b) a zoom-in on 13 – 17 November 2008 and (c) the Hg^{o}-wind speed correlation with r^2=0.18, slope = 3.7 ppqv per 1 m s^{-1} for the zoom-in period. The time axis is shown in Universal Time (UTC).

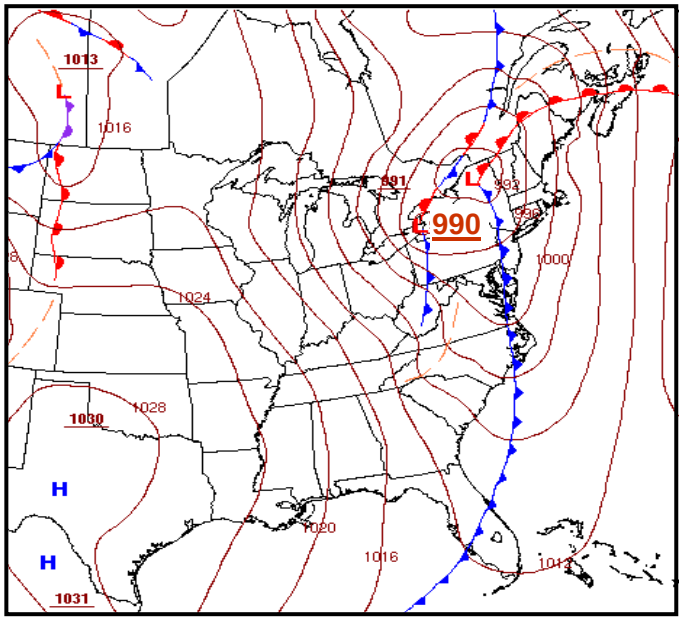

Figure 2. Surface analysis from the Hydrometeorological Prediction Center (http://www.hpc.ncep.noaa.gov/) for 0000 UTC November 16, 2008. Sea level pressure is contoured with reddish brown lines every 4 hPa. Cold (blue), warm (red), and occluded (purple) frontal positions are also shown and central pressures (hPa) of highs and lows are shown with underlined numbers.

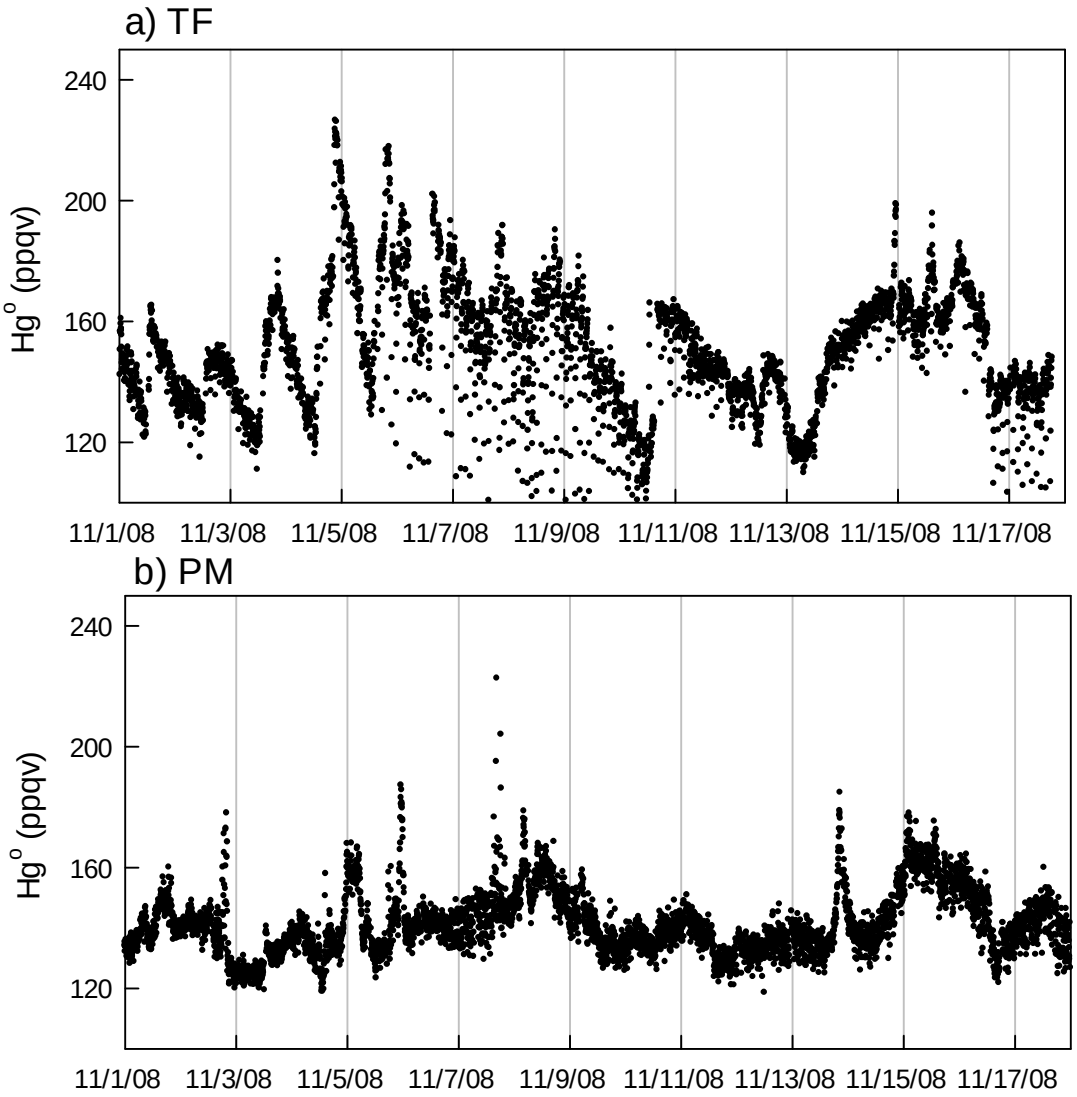

Figure 3. Hg^o mixing ratios at TF (coastal) (a) and PM (inland) (b) during the time period of 1 – 17 November 2008.

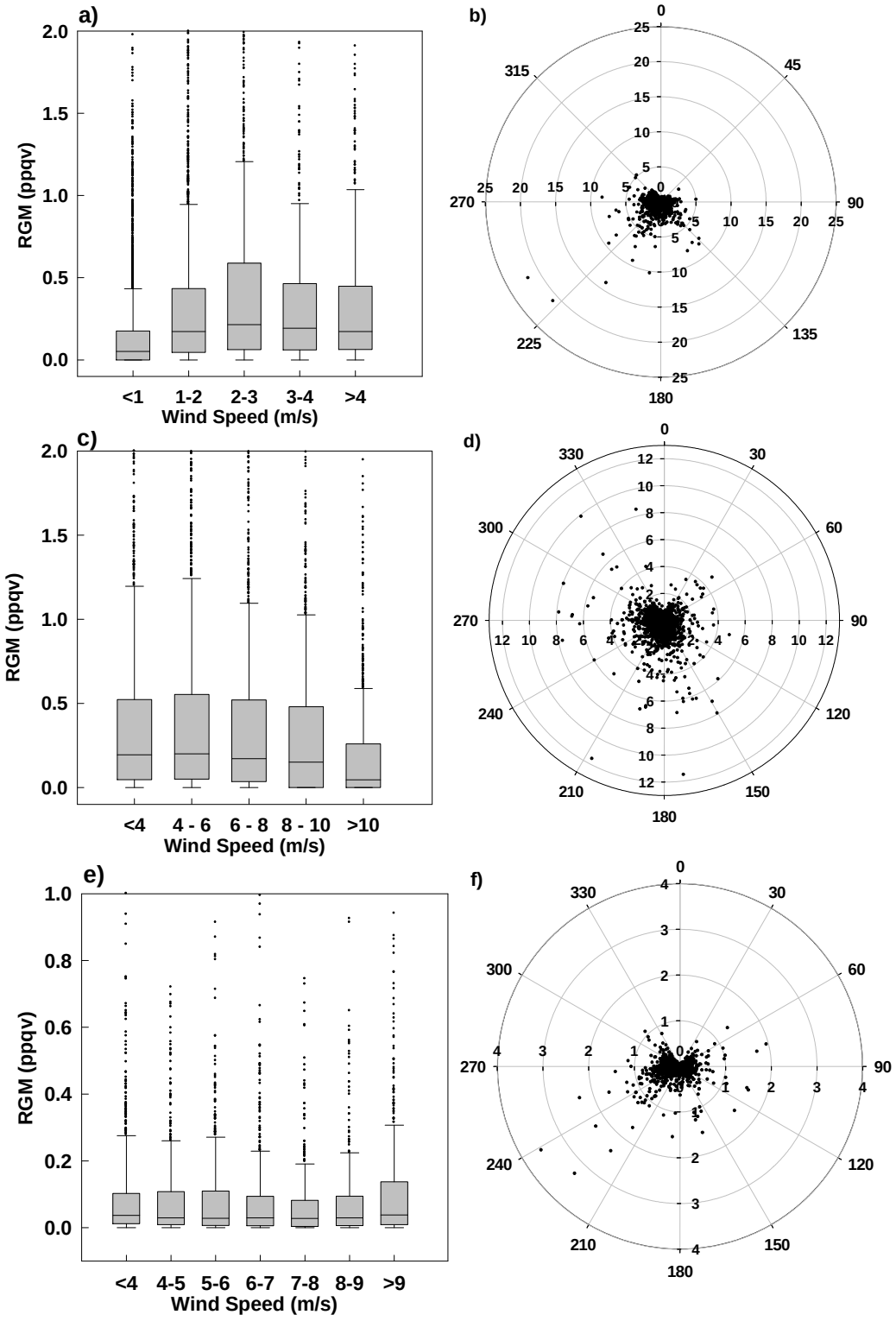

Figure 4. RGM mixing ratios versus wind speed and direction at TF (coastal) (a,b), AI (marine) (c,d), and PM (inland) (e,f). The number labels on the range rings in wind roses represent mixing ratios in tenths of ppqv.

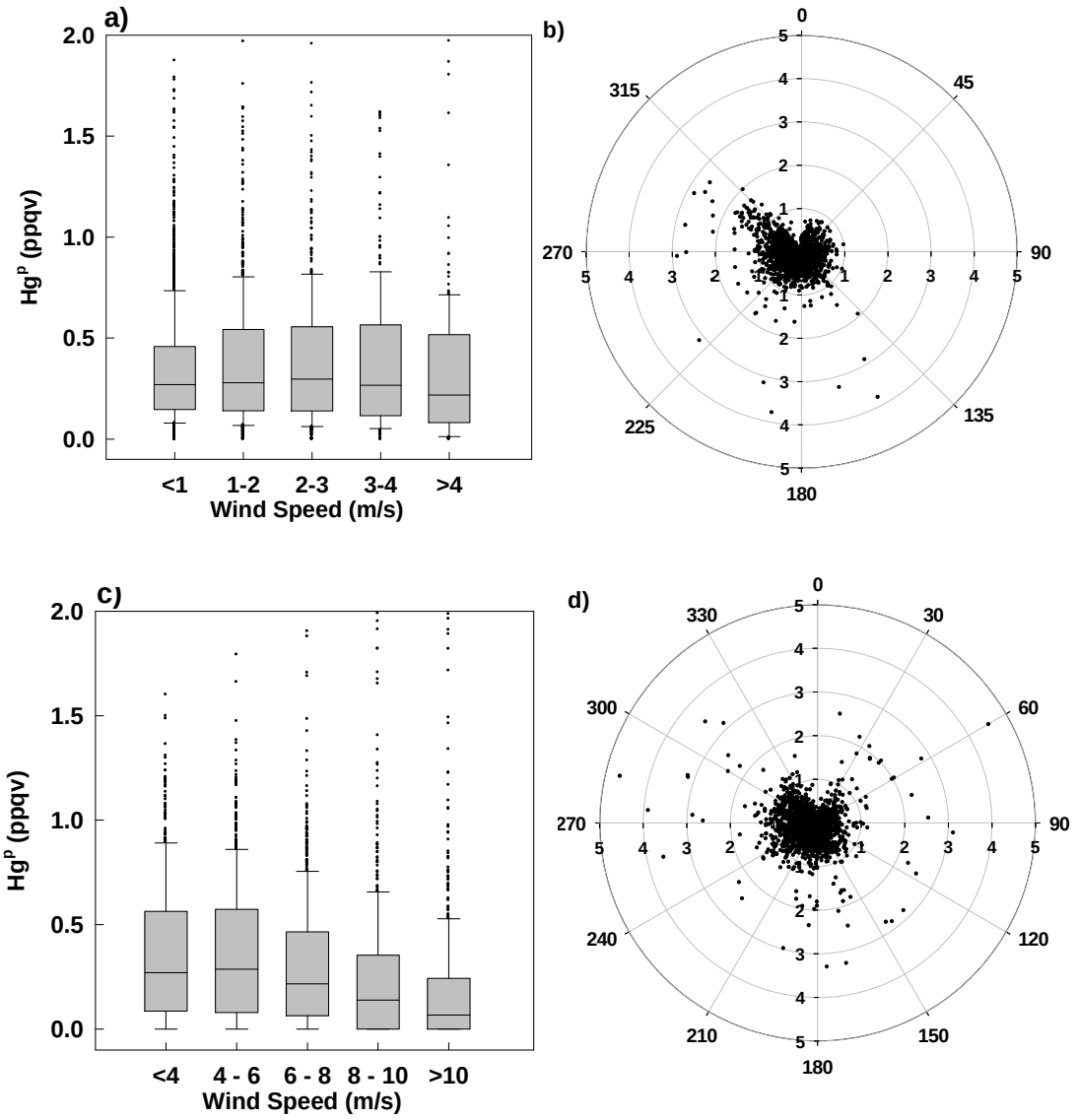

Figure 5. Hg^P mixing ratios versus wind speed and wind direction at TF (coastal) (a,b) and AI (marine) (c,d). The number labels on the range rings in the wind roses represent mixing ratios in tenths of ppqv.

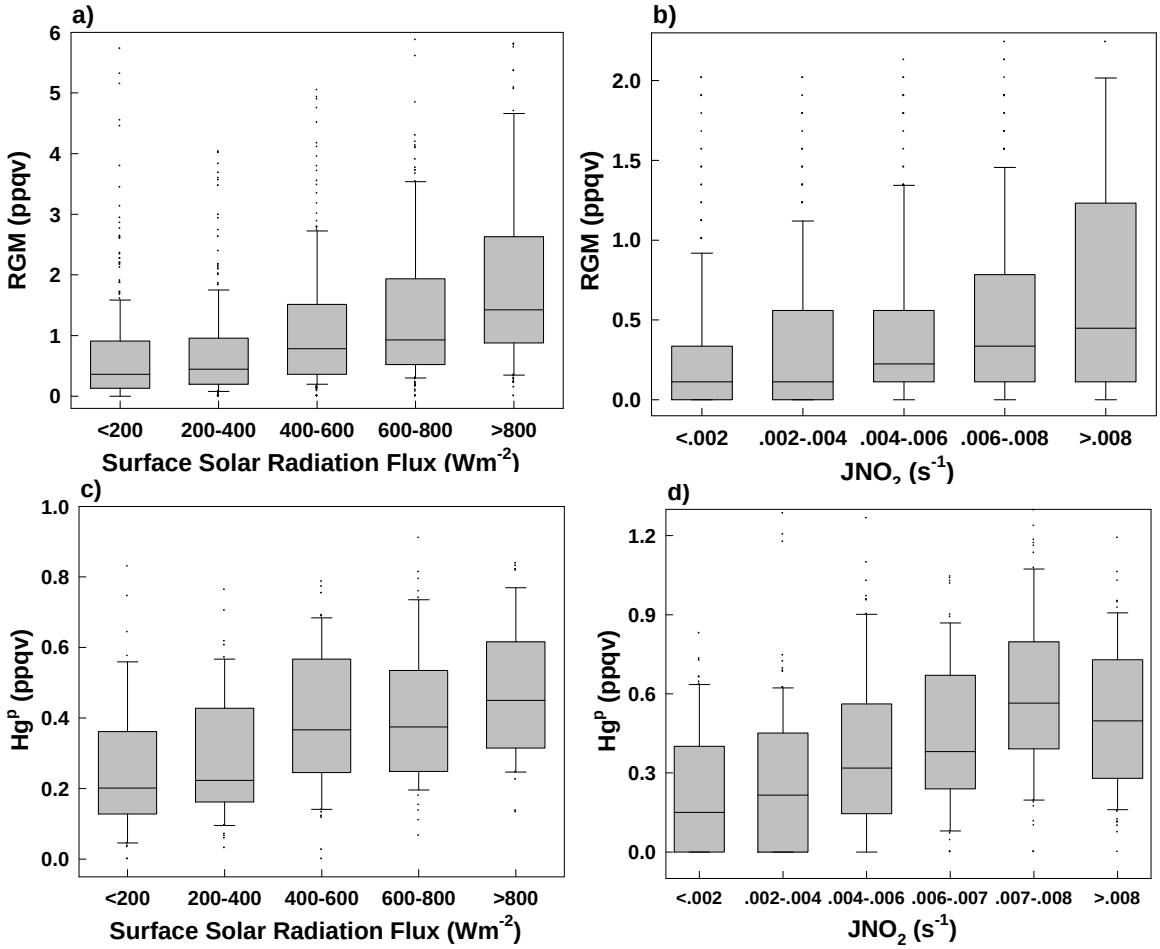

Figure 6. a) RGM versus surface solar radiation flux at TF (coastal) in spring, b) RGM versus $j\mathrm{NO_2}$ at AI (marine) in spring and summer, c) $\mathrm{Hg^P}$ versus surface solar radiation flux at TF (coastal) in summer, and d) $\mathrm{Hg^P}$ versus $j\mathrm{NO_2}$ at AI (marine) in summer. Only daytime data were used.

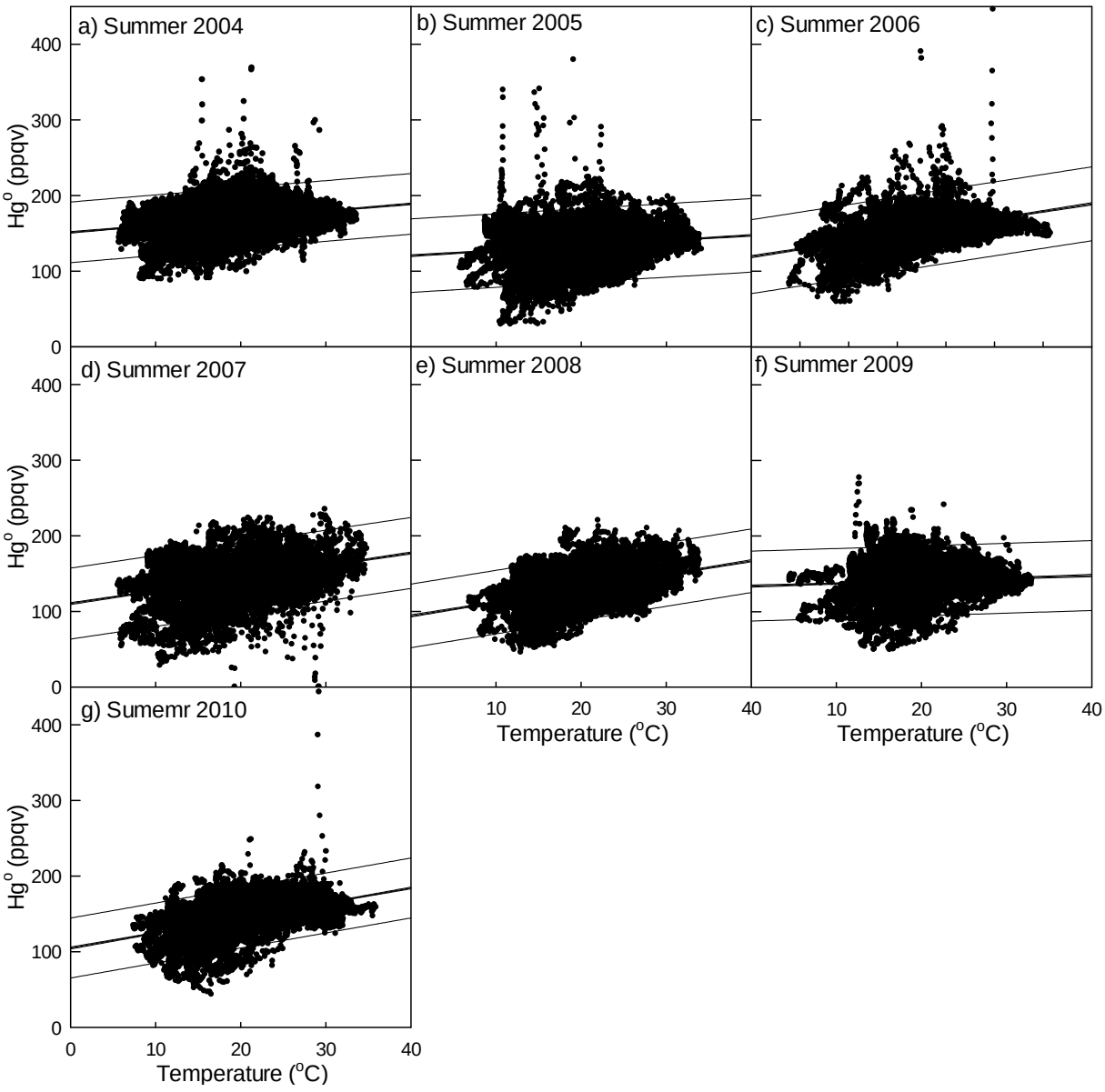

Figure 7. Mixing ratios of Hg^o versus temperature in summers of 2004 – 2010 at TF (coastal). The lines indicate the 95% confidence interval.

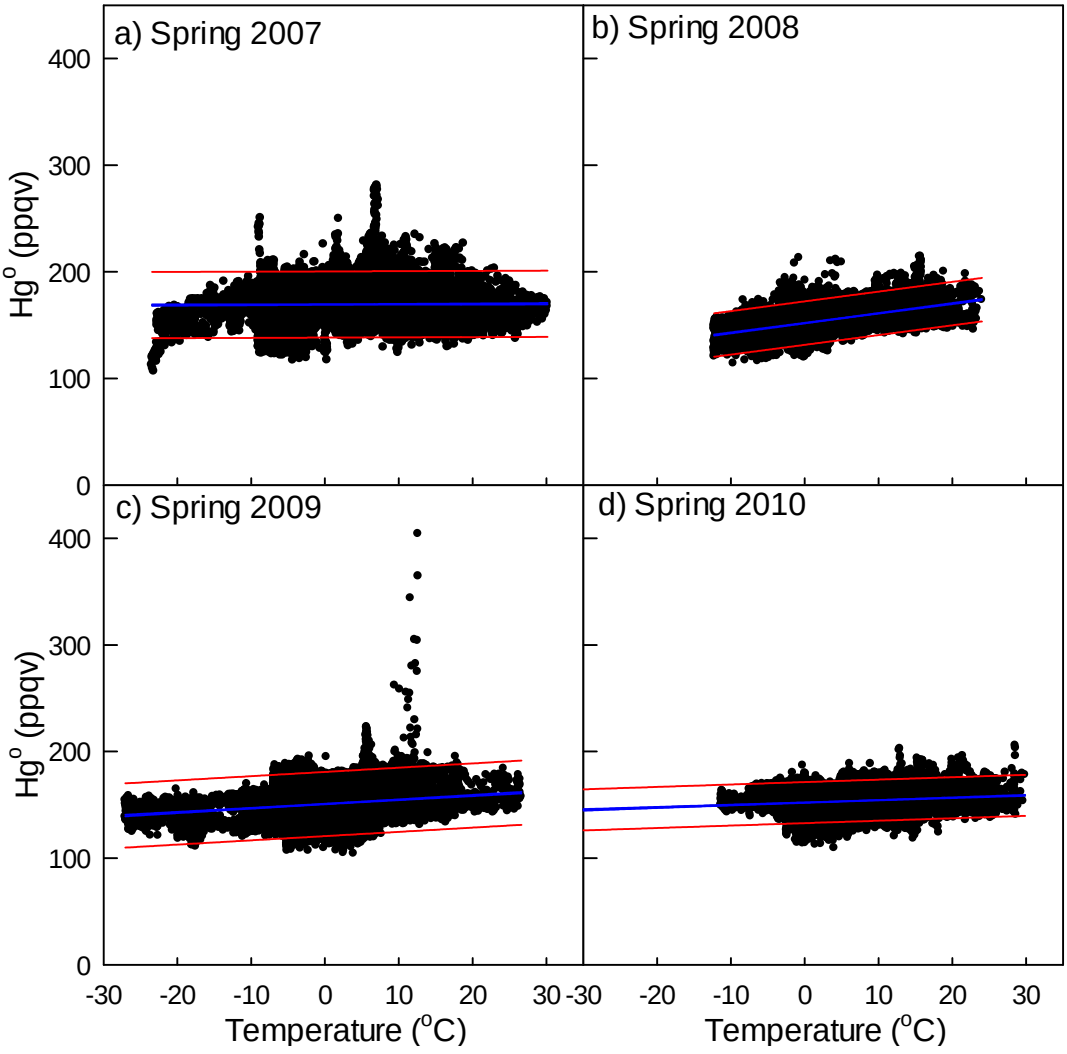

Figure 8. Mixing ratios of Hg^o versus temperature in springs 2007 – 2010 at PM (inland). The lines indicate the 95% confidence interval.

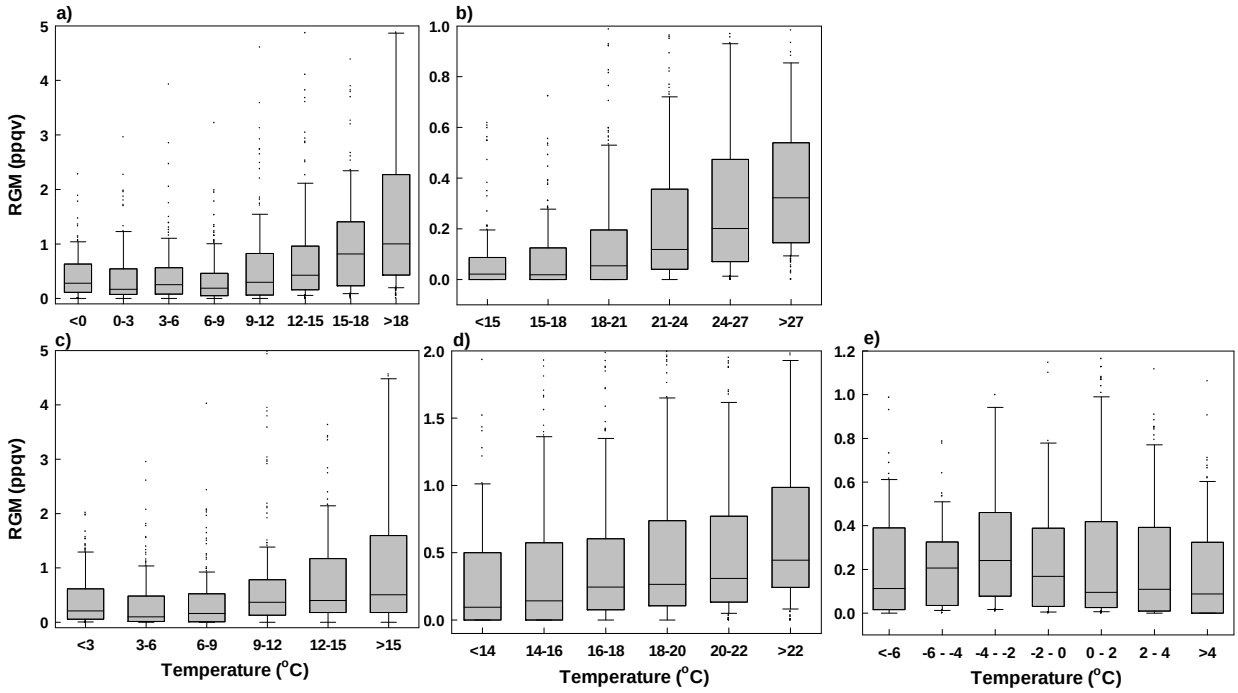

Figure 9. Daytime mixing ratios of RGM versus temperature at TF (coastal) in (a) springs and (b) summers 2003 – 2010, at AI in (c) springs, (d) summers, and (e) winters 2007 – 2010.

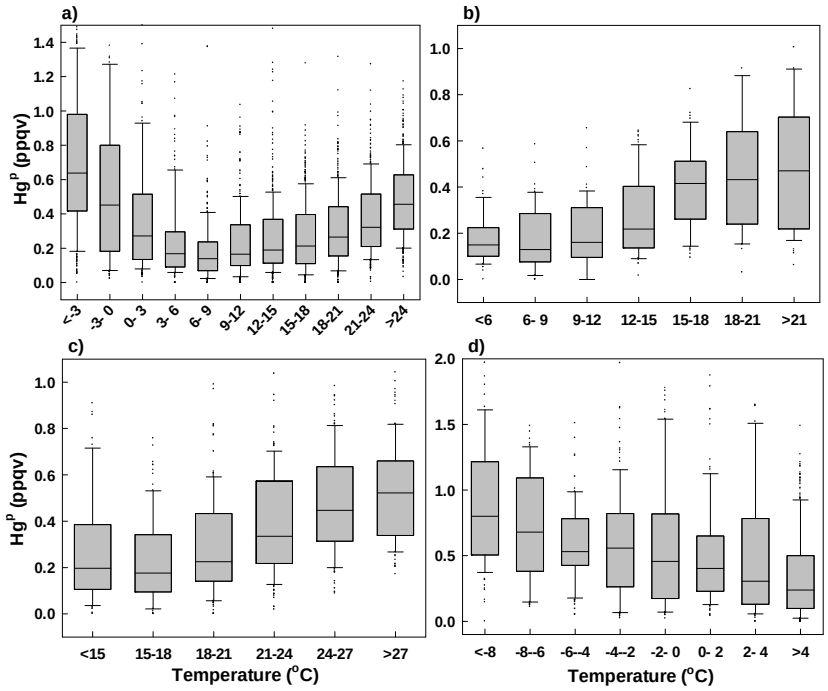

Figure 10. Relationships between Hg^P and temperature at TF (coastal) for (a) all seasons, (b) daytime springs, (c) daytime summers, and (d) winters during January 2009 – August 2010.

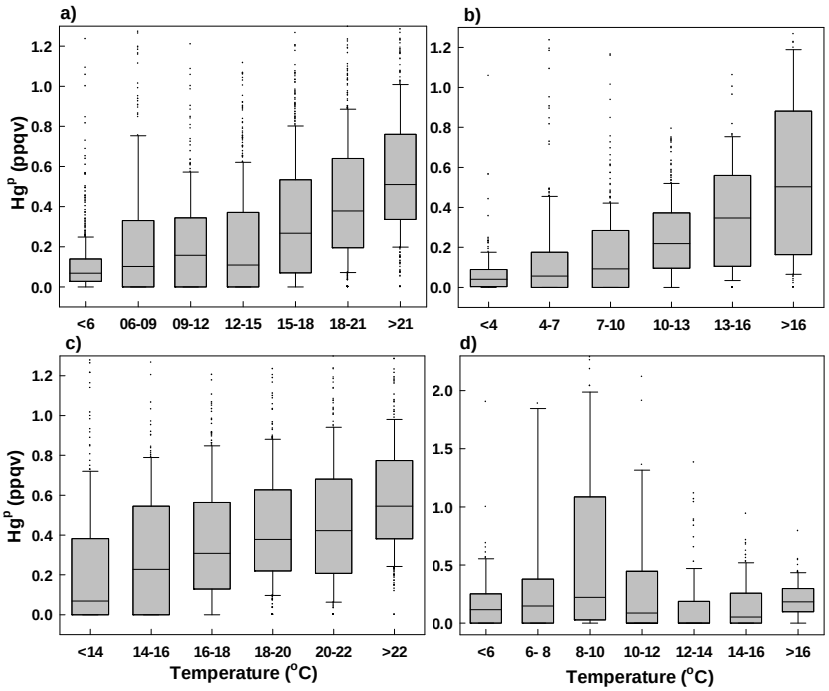

Figure 11. Relationships between Hg^P and temperature at AI (marine) for (a) all seasons, (b) springs, (c) summers, and (d) falls during April 2009 – August 2010. There was only one month data for the winter season during the entire study period.

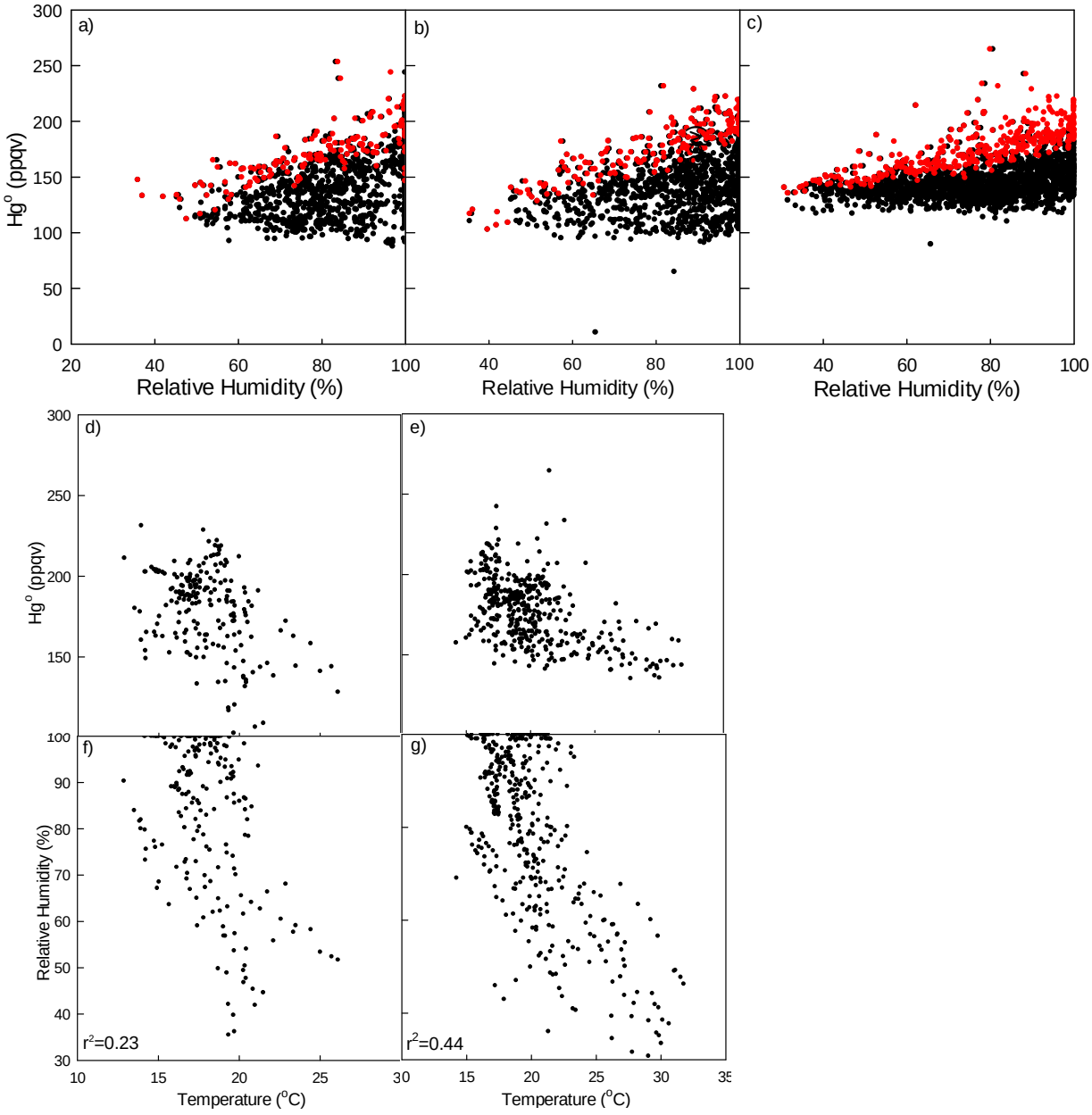

Figure 12. Relationships between Hg^o and relative humidity at AI (marine) for summers (a) 2007, (b) 2008, and (c) 2010. Points forming the linear upper boundary are highlighted in red. Relationships between Hg^o and temperature (d,e), temperature and relative humidity (f,g) for the points in the upper boundary in summers 2008 and 2010.

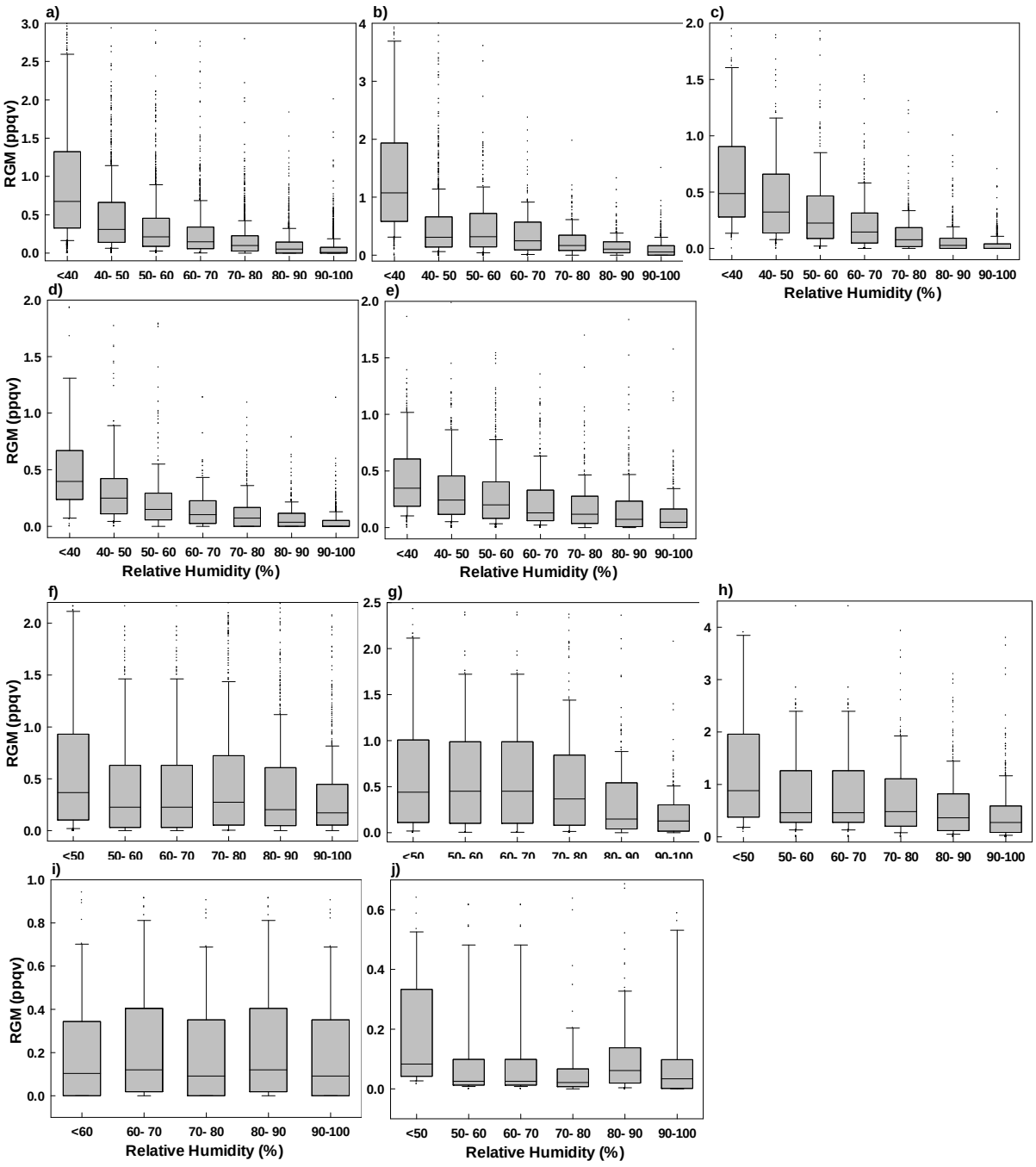

Figure 13. Relationships between RGM and relative humidity at TF (coastal) (a-e) and AI (marine) (f-j) for all seasons (a,f), springs (b,g), summers (c,h), falls (d,i), and winters (e,j).

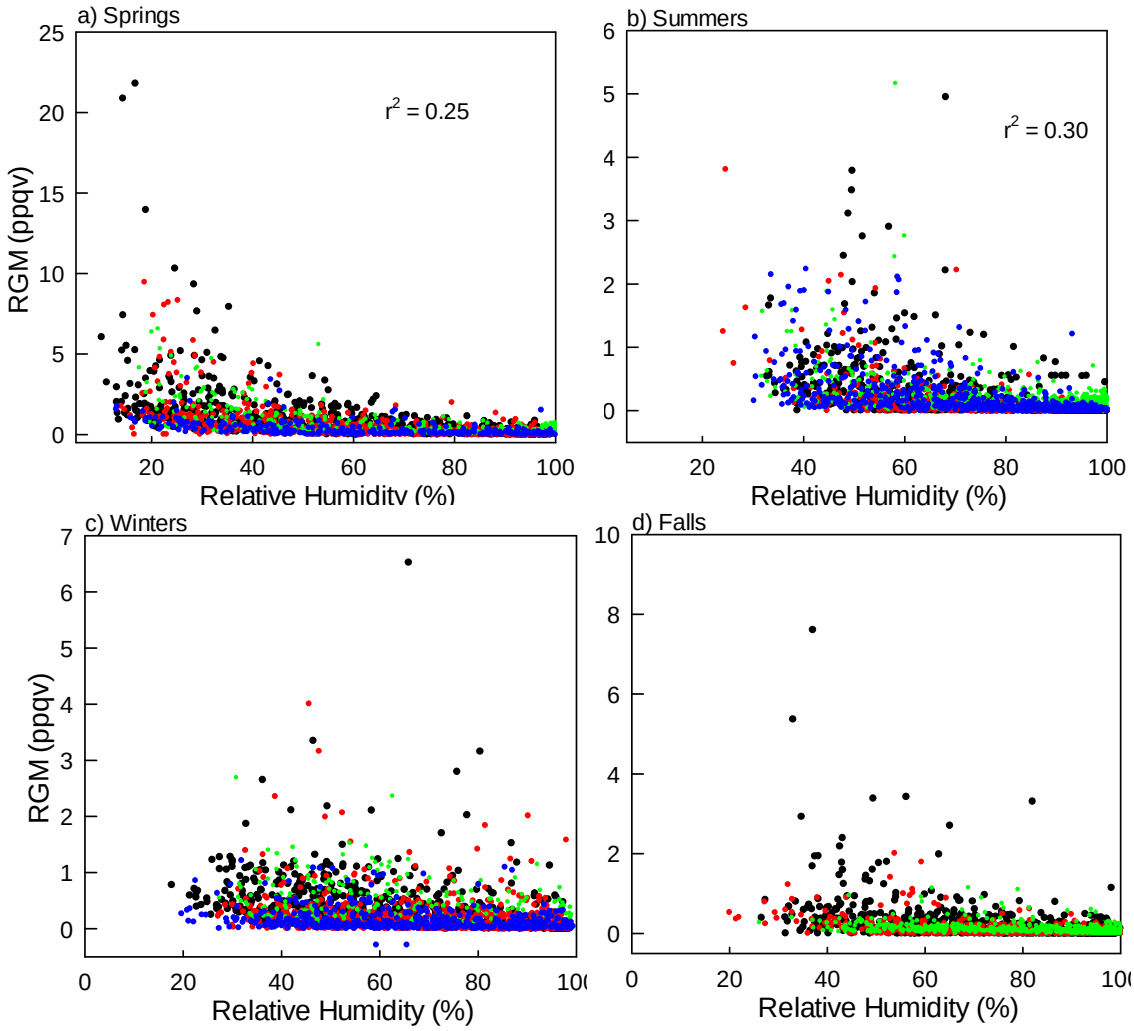

Figure 14. Relationships between RGM and relative humidity at TF (coastal) in (a) springs, (b) summers, (c) falls, and (d) winters with data from 2007 in black, 2008 in red, 2009 in green and 2010 in blue.

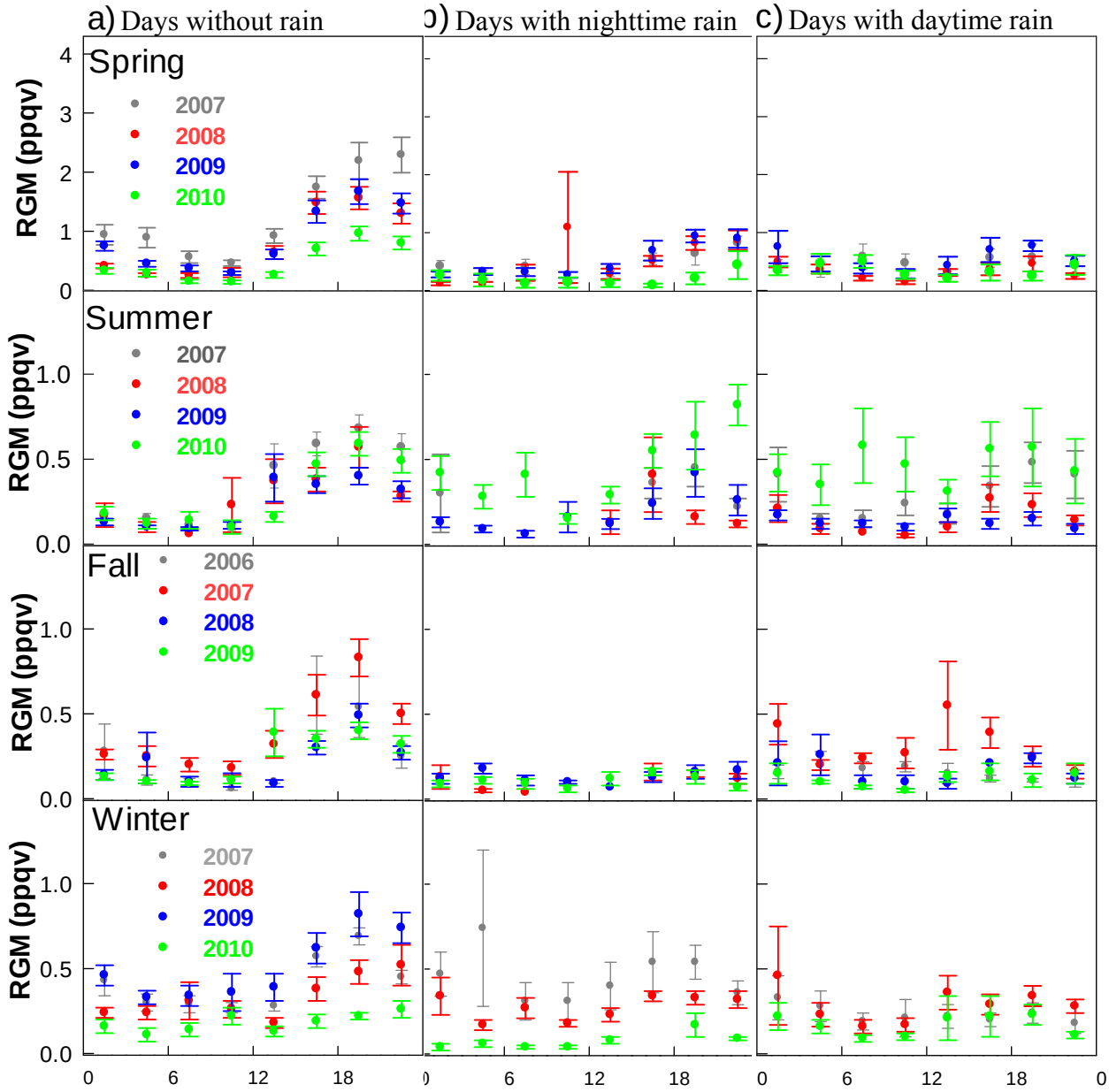

Figure 15. Diurnal cycles of RGM at TF (coastal) averaged over days without rain (a), days with nighttime rain (b), and days with daytime rain (c) for all seasons during 2006 – 2010. It should be noted that there were data in February only in winter 2009 and there were too few data for conditions in (b) and (c) in winter to be presented for comparison. Similarly there were data in November only for fall 2006 and there were insufficient data in Fall 2006 for (b). Precipitation in winter includes rain and snow.

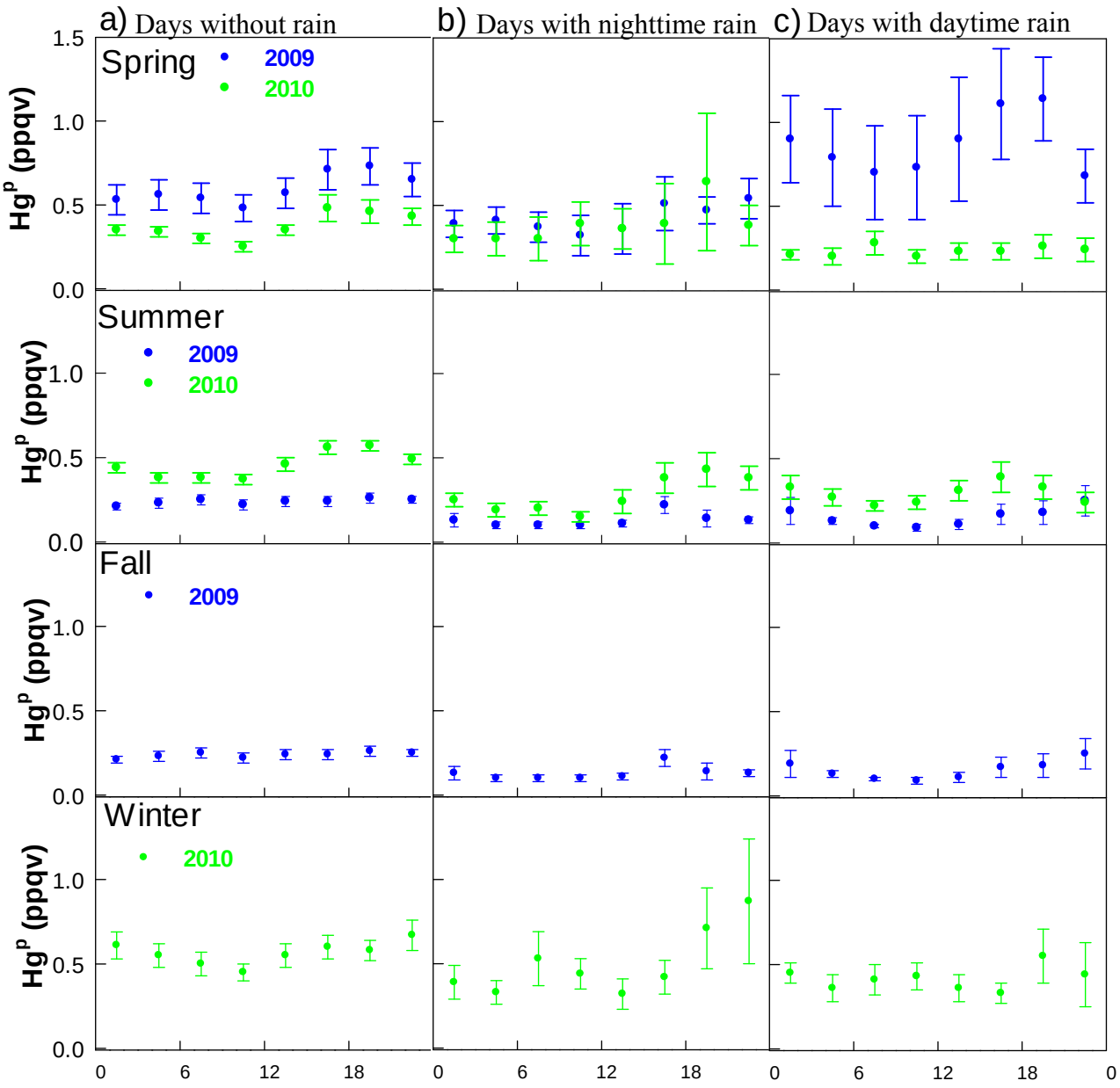

Figure 16. Diurnal cycles of Hg^P at TF (coastal) averaged over days without rain (a), days with nighttime rain (b), and days with daytime rain (c) for all seasons during 2009 – 2010. Precipitation in winter includes rain and snow.

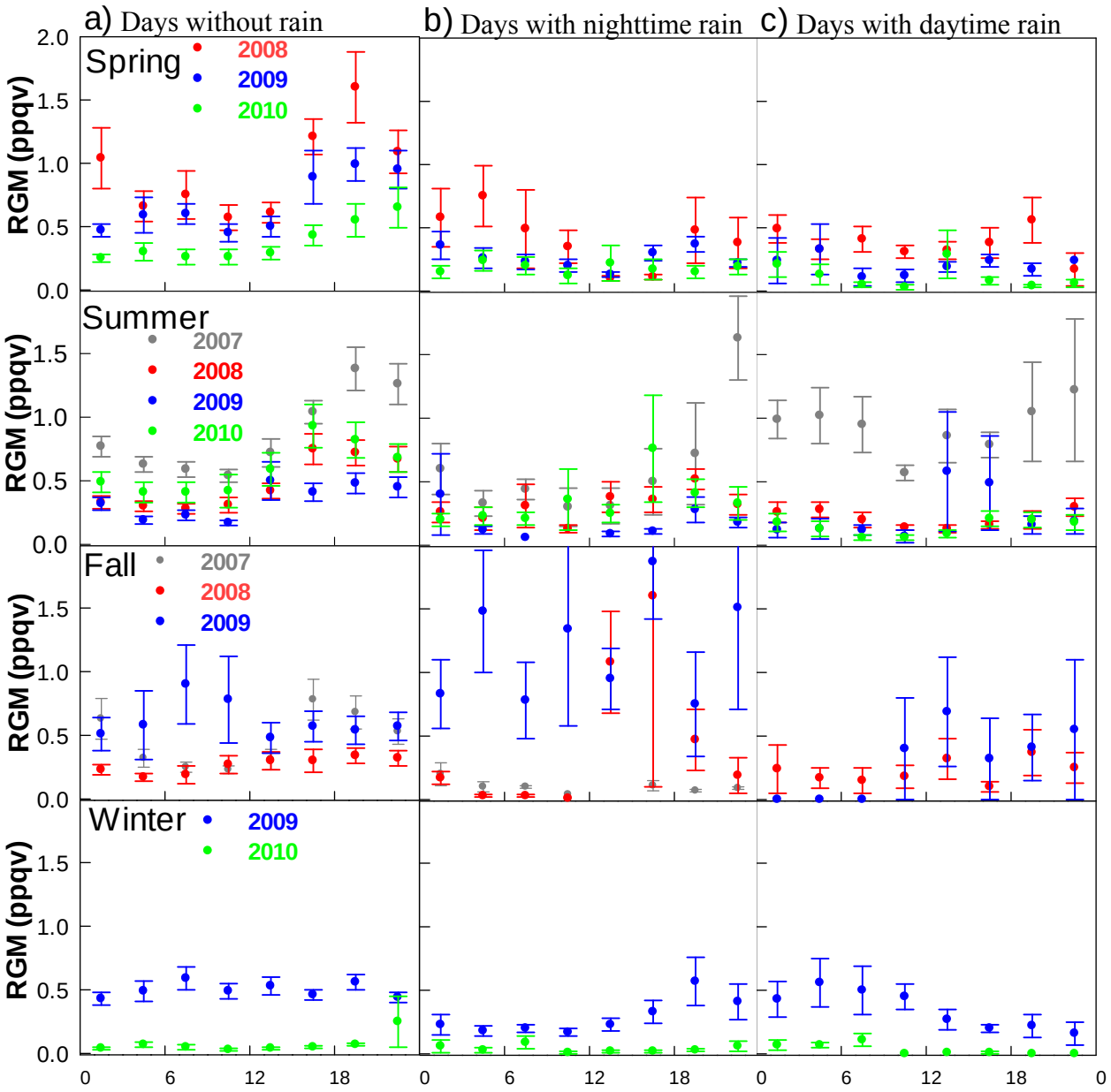

Figure 17. Diurnal cycles of RGM at AI (marine) averaged over days without rain (a), days with nighttime rain (b), and days with daytime rain (c) for all seasons during 2007 – 2010. Precipitation in winter includes rain and snow.

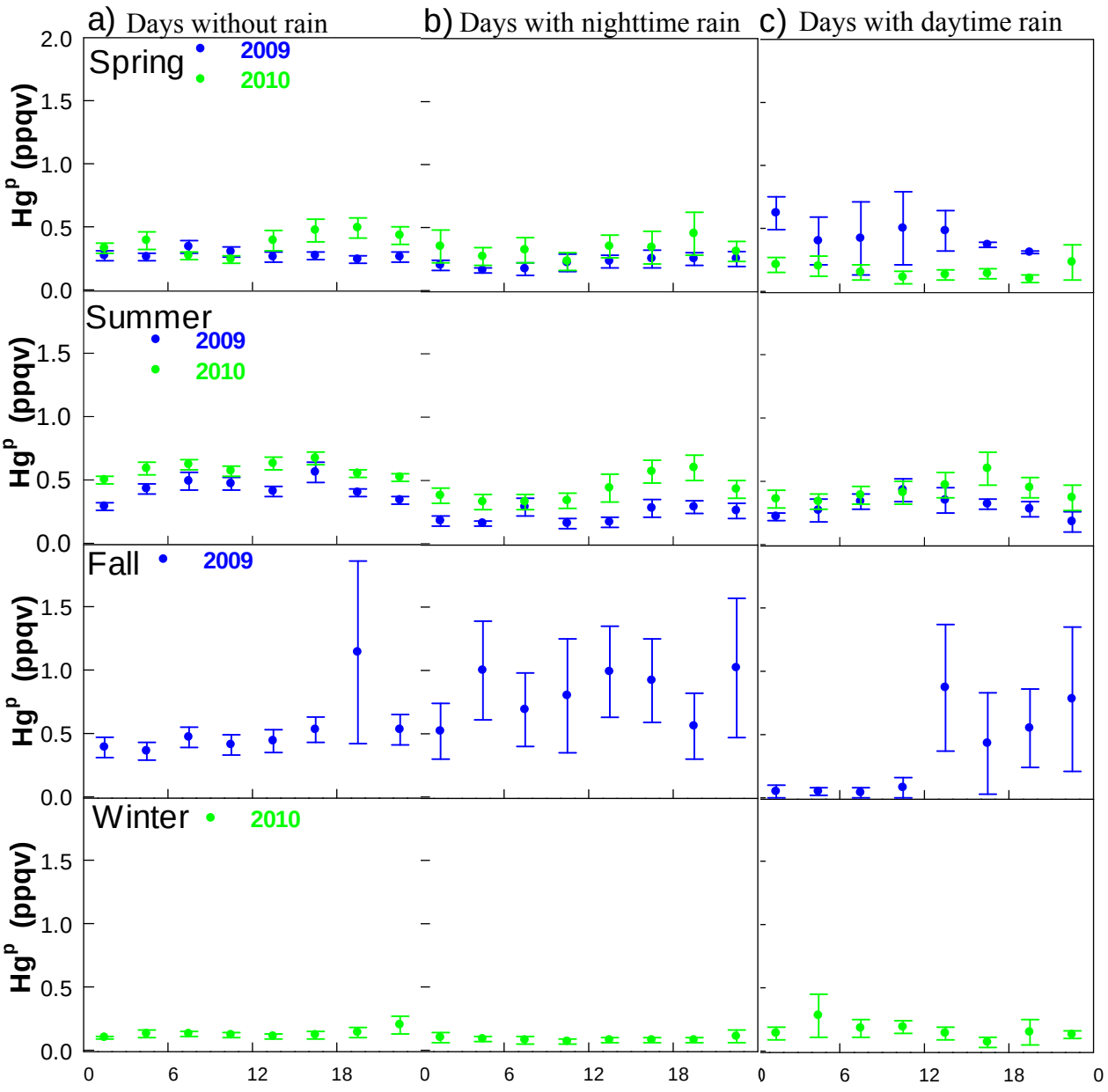

Figure 18. Diurnal cycles of Hg^P at AI (marine) averaged over days without rain (a), days with nighttime rain (b), and days with daytime rain (c) for all seasons during 2009 – 2010. Precipitation in winter includes rain and snow.